



# Formation mechanism and accumulation model of primary condensate reservoir in Hailar Basin, NE China

Jingsheng Li<sup>1,3,4</sup> · Congsheng Bian<sup>2</sup> · Zhongquan Li<sup>1</sup> · Xiaodong Zhang<sup>3,4</sup> · Haibo Wu<sup>3,4</sup> · Wei Peng<sup>3,4</sup> · Yuhui Deng<sup>3,4</sup> · Wenjing Shen<sup>3,4</sup>

Received: 5 February 2021 / Accepted: 6 January 2022 / Published online: 9 May 2022  
© Saudi Society for Geosciences 2022

## Abstract

The condensate reservoir of  $K_1n^2$  in the Hailar Basin is generated from the coal measure strata and has high gas-oil ratio. Although the condensate reservoir has been discovered in the late 90 s, there is still vague about the formation mechanism and accumulation model. By analyzing the hydrocarbon generation and expulsion process of the coal measure strata, dissecting the evolution of temperature and pressure of oil and gas reservoirs with reference to the paleotemperature recovered by apatite fission track, and deeply discussing the mechanism and law of oil and gas accumulation, this paper points out that coal measure source rocks have the characteristics of “early generation and early expulsion, continuous hydrocarbon generation with the predominant gas generation,” which lays a material condition for the formation of condensate oil and gas. A stable temperature and pressure system was formed by the sealing of the thick mudstone of the  $K_1n^1$  overlying the  $K_1n^2$  with the abnormal low pressure, which provides the most ideal temperature and pressure conditions. Two stages of fault system are developed in the Hailar Basin. The fault system formed in the fault depression stage is mainly developed in the strata of the  $K_1n^2$  and below. The fault system in rift stage is mainly developed in the strata of the  $K_1n^2$  and above, and most of it disappears in the thick mudstone of the  $K_1n^1$ , effectively preventing the upward loss of oil and gas. Oil and gas are mainly distributed in the strata of the  $K_1n^2$ . The coal measure strata of the  $K_1n^2$  have the characteristics of “integration of source and reservoir.” The matching of structure and high-quality reservoir controls the formation of oil and gas reservoir with the oil and gas most enriching at the structural high point. By analyzing the controlling factors of oil and gas reservoir formation, three oil and gas reservoir forming models are established, including fault step type in steep slope zone, anticline type in steep slope zone, and fault step type in gentle slope zone. Some favorable exploration areas, such as the south sag of Huhehu depression, the north sag of Hulunhu depression, the north sag of Yimin depression and the South sag of Chagannuoer depression, are determined and the exploration works should be focused on the hydrocarbon expulsion center of coal rock.

**Keywords** Condensate reservoir · Hailar Basin · Coal measure strata · Fault system · Accumulation model

Responsible Editor: Santanu Banerjee

✉ Congsheng Bian  
biancongsheng@126.com

- <sup>1</sup> College of Earth Sciences, Chengdu University of Technology, Chengdu 610059, Sichuan, China
- <sup>2</sup> Research Institute of Petroleum Exploration and Development, Petrochina, Beijing 100083, China
- <sup>3</sup> Heilongjiang Key Laboratory of Tight Oil and Mudstone Oil Accumulation Research, Daqing 163712, Heilongjiang, China
- <sup>4</sup> Exploration and Development Research Institute, Daqing Oilfield Ltd Co., Daqing 163712, Heilongjiang, China

## Introduction

Condensate reservoir is a special type of natural gas reservoir, which contains condensate oil under the original formation conditions, with its temperature between the critical temperature and the highest condensate temperature (Zhou et al. 1996; Nasriani et al. 2014; Ferreira et al. 2018; Wang et al. 2021). The basic characteristic of condensate reservoir is that natural gas and condensate oil are in a single gas phase under formation conditions, and conform to the law of retrograde condensation within a certain pressure range (Yang and Zhu 2013). As a special oil and gas resource (Tong et al. 2018), condensate reservoir has been discovered for more than 100 years. At present, there are more

than 100 large condensate oil and gas fields discovered in the world (Yang et al. 2010), including Sichuan, Bohai Bay, Dagang, North China, Tarim and Beibu Gulf Basin (Zhou et al. 1996; Huang et al. 2003; Ping et al. 2012; Zhu et al. 2012; Yang and Zhu 2013; Cao et al. 2017; Wei et al. 2017; Liu et al. 2018; Xue and Li 2018), and more than 20 discovered in Tarim Basin alone (Li et al. 2013; Su et al. 2018). The following conditions must be met for the formation of condensate reservoir: firstly, the formation is deeply buried until the formation temperature reach between the critical temperature and the critical condensation temperature of hydrocarbons, as well as the formation pressure exceeding the leakage point pressure of this temperature. Secondly, the quantity of gas must surpass that of liquid, that is, natural gas accounts for the vast majority underground in condensate reservoir. In addition, stable temperature and pressure system is necessary for condensate reservoir, which mostly generated by coal measure strata, as well as the high maturity source rocks.

The discovered hydrocarbon reservoirs in the Hailar Basin are mainly distributed in the Urxun and Beier depressions in the middle and south of the basin, which mainly produced light oil and medium oil. There are heavy oil reservoirs in the Bayanhushu depression in the western part of the basin. In addition to these conventional reservoirs, the Hailar Basin has also discovered condensate reservoirs, which mainly distributed in Huhehu depression in the east of the basin and Hulunhu depression in the west of the basin. The discovered condensate reservoirs in the Hailar Basin are directly related to coal measure source rocks (Lu et al. 2010; Shen 2010; Cui et al. 2018; Chen 2015), but their buried depth are generally less than 3000 m. However, source rocks in that depth are generally in the wet gas stage, which are similar to the geological conditions for conventional hydrocarbon. So far, the geological conditions and distribution law of condensate reservoirs are still vague, which influence the oil and gas exploration process. By research on the geological characteristics of condensate reservoir in the Hailar Basin, this paper establishes the accumulating mechanism and forming models of condensate reservoir, which will help to the oil and gas exploration deployment of condensate reservoir in the Hailar Basin and obtain greater industrial oil and gas discoveries.

## Geological setting

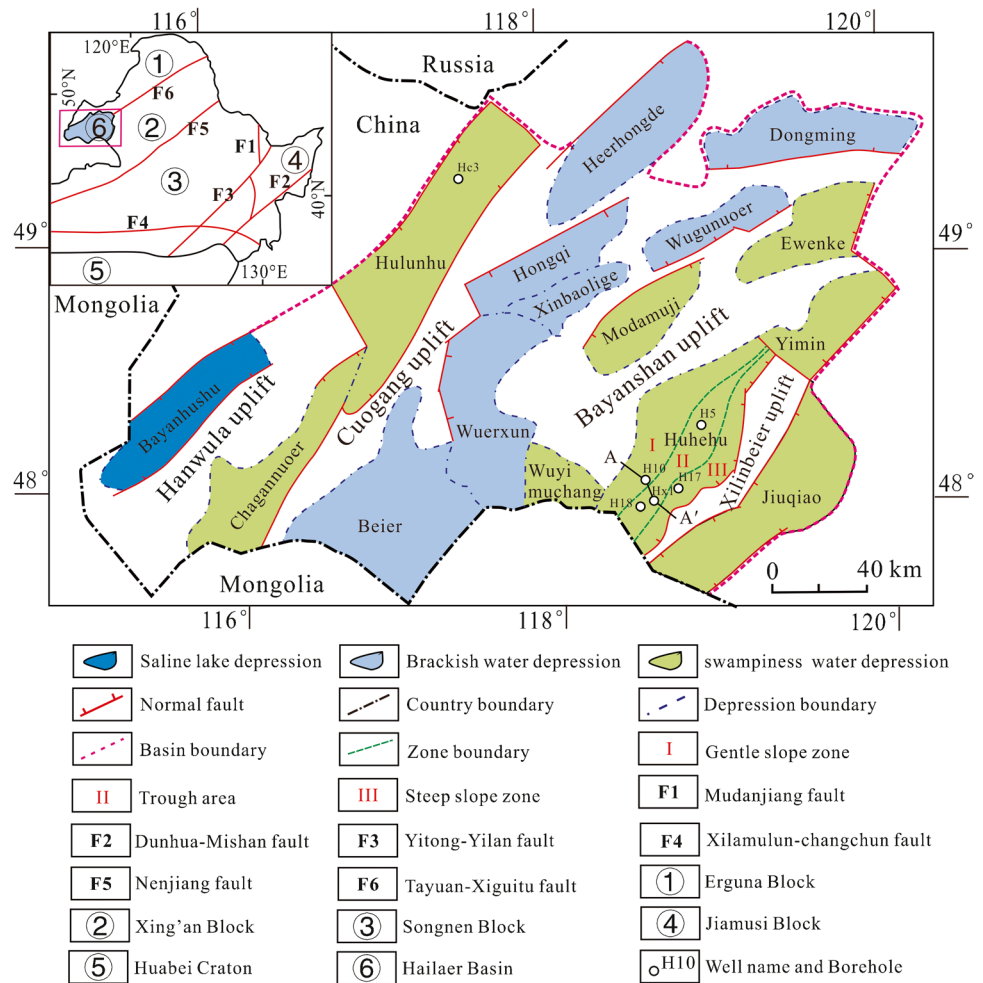
The Hailar Basin is located in the northernmost part of Northeast China, bordering Russia to the north and Mongolia to the west and southwest, with the area of  $4.4 \times 10^4$  km<sup>2</sup>. The Hailar Basin is a Late Mesozoic-Paleogene fault-depression basin developed on the Hercynian fold basement (Chen et al. 2007). The basin is composed of 16 relatively

independent depressions (Fig. 1), with a structural pattern of three depressions and two uplifts. There are six formations developed on the basement of the basin: the Jurassic Tamulangou Formation (Li 2013), the Lower Cretaceous Tongbomia Formation ( $K_1t$ ), Nantun Formation ( $K_1n$ ), Damoguaihe Formation ( $K_1d$ ) and Yimin Formation ( $K_1y$ ), and the Upper Cretaceous Qingyuangang Formation ( $K_2q$ ) (Fig. 2). The basin evolution process can be divided into three periods, there are rifting period (Tamulangou-Tongbomia formation-Nantun formation deposition period), rifting-depression period (Damoguaihe formation-Yimin formation deposition period), and depression period (Qingyuangang formation), and the main source-reservoir assemblages were developed in the first and second members of the Nantun Formation ( $K_1n^1$  and  $K_1n^2$ ) during the rifting period. According to the types of lake water environment during the main source rocks developing period, the 7 depressions located in the middle of the basin belong to brackish basin. The organic matter type is Type II. The Bayanhushu depression in the west of basin is a saltwater basin, the organic matter type is Type I, and the remaining 8 depressions are freshwater basins, and the organic matter type is Type II-III (Fig. 1). The discovered condensate reservoirs are distributed in the Huhehu and Hulunhu depressions. During the second members of the Nantun Formation ( $K_1n^2$ ), it is always swamped basin, which belongs to the typical coal-measure stratigraphic deposits.

The braided river delta deposition system is developed in the gentle slope zone of the swamped basin, the fan delta deposition system is developed in the steep slope zone, and the shore-shallow lake is the main sub-environment in the depression area. Studies on the relationship between sedimentary facies and physical properties show that the plains and frontal sand bodies of the fan delta and braided river delta have good physical properties, and they are all good reservoirs. Vertically, with the increase of buried depth and the strengthening of diagenesis, the porosity of the reservoir decreases sharply, but secondary dissolved pores develop. The physical properties of the upper reservoir of  $K_1n^2$  are the best. The porosity range is 3.6–18.8%, with an average of 11.3%, and the permeability is  $0.01 \sim 53.10 \times 10^{-3} \mu\text{m}^2$ , with an average of  $1.09 \times 10^{-3} \mu\text{m}^2$ , which belongs to the medium–low porosity and ultra-low permeability reservoir.

The condensate reservoirs in the Hailar Basin mainly come from the coal-measure source rocks of  $K_1n^2$  (Lu et al. 2010; Shen 2010; Cui et al. 2018). According to the statistics of 123 samples of dark mudstone and 44 samples of coal seam coal rock in  $K_1n^2$  of Huhehu depression, the results show that the coal-measure source rocks of  $K_1n^2$  in Huhehu depression include dark mudstone and coal seams (Table 1). The organic carbon of the dark mudstone is distributed between 0.52 and 7.17%, with an average of 2.71%, and the chloroform pitch “A” is distributed between 0.0077

**Fig. 1** Simplified geological map of the Hailar Basin and sampling wells location with crossing seismic sections



and 1.0659%, with an average of 0.1233%, the hydrocarbon generation potential is 0.09 ~ 13.98 mg/g, with an average of 4.23 mg/g. The organic carbon of coal rocks is distributed between 23.00 and 79.06%, with an average of 55.19%, chloroform pitch “A” is distributed between 0.0042 and 1.3840%, with an average of 0.6002%, and the hydrocarbon generation potential is 26.72 ~ 324.3 mg/g, with an average of 111.59 mg/g. The type of organic matter is II2 ~ III, Ro is distributed between 0.50 and 1.67%, which is in the mature-high mature stage.

## Samples and methods

### Fluid characteristic analysis and carbon isotope analysis experiment

In order to understand the fluid characteristics and hydrocarbon source of condensate reservoir, the carbon isotope of condensate gas is analyzed. In this study, 8 gas samples and 3 oil samples from wells H10, H18, H17, HC3, and HX1 were taken for fluid characteristic analysis. The gas samples

were tested by gc6890 gas chromatograph. The sample depth and analysis results are shown in Table 2. The test method of gas sample is as follows: as the sample is sent to the injector, it is carried by the carrier gas into the packed column or capillary column. Due to the differences of boiling point, polarity, and adsorption coefficient of each component in the sample, each component is separated in the column, and then the detector connected behind the column detects each component in sequence according to the physical and chemical properties of the components. Finally, the converted electrical signal is sent to the chromatographic workstation, and the chromatographic workstation records and analyzes the gas chromatogram of each component, so as to obtain the analysis results of each component. The depth and analysis results of three condensate samples are shown in Table 3. The density of crude oil is 20 °C and the kinematic viscosity is tested in 50 °C. In addition, in order to clarify the origin of condensate gas, three gas samples are selected for carbon isotope analysis of natural gas components. The analysis results are shown in Table 2. It can be seen from the analysis results that the carbon isotope value gradually becomes heavier with the increase of gas carbon number.

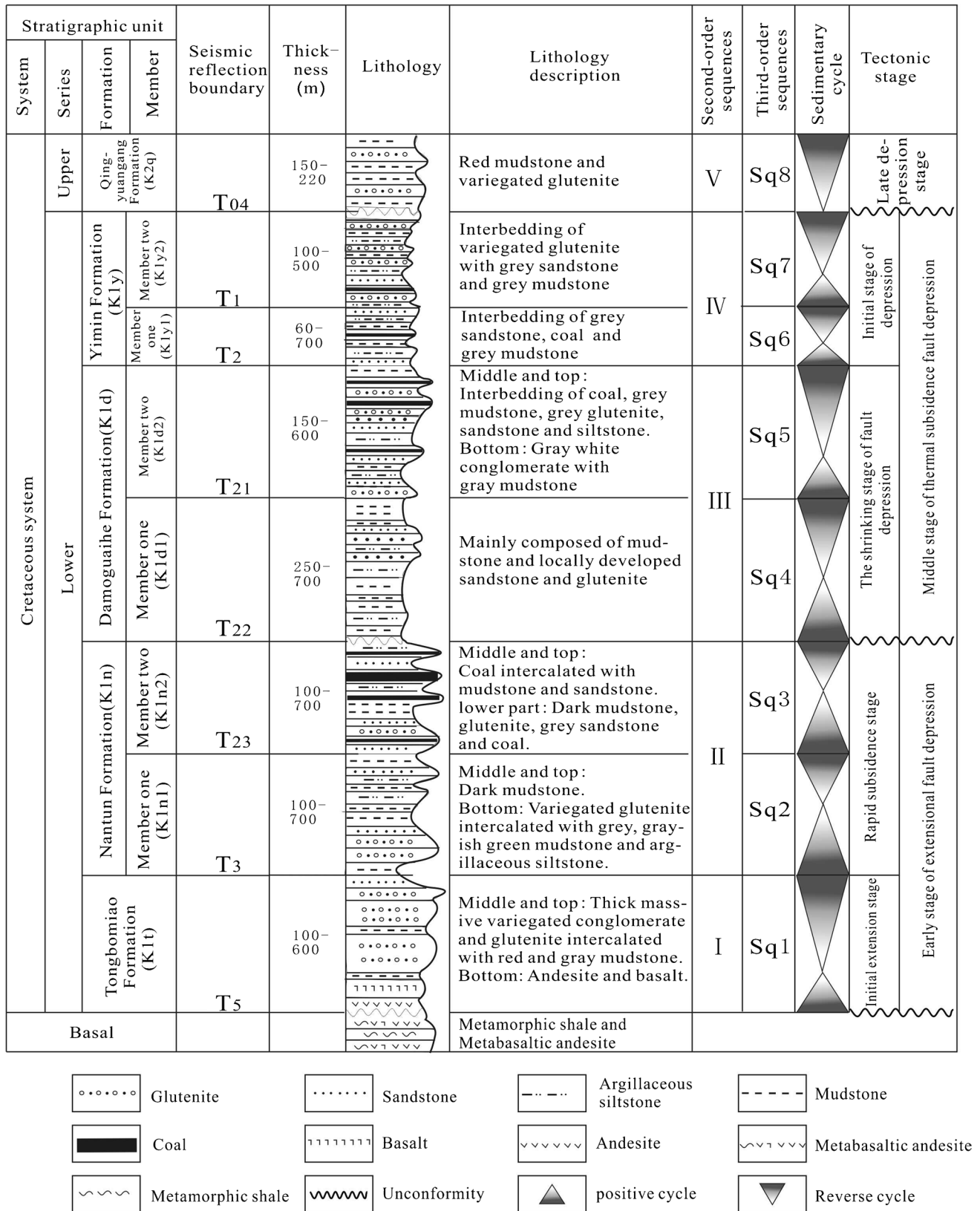


Fig. 2 Comprehensive stratigraphic column of Huhehu depression

**Table 1** Statistical table of organic matter abundance of mudstone and coal in K<sub>1n</sub><sup>2</sup> of Nantun Formation in Huhehu sag (some data from reference of Zhang (2014) and Chen 2014)

Lithology	TOC (%)	Chloroform asphalt "A" (%)	Hydrocarbon generation potential (mg/g)	Ro (%)
Mudstone	0.522–7.167 2.708/123	0.0077–1.0659 0.1233/62	0.09–13.98 4.228/120	0.50–1.67
Coal	23–79.061 55.190/44	0.0042–1.384 0.6002/22	26.715–324.37 111.587/43	

**Table 2** The carbon isotopes of natural gas of K<sub>1n</sub><sup>2</sup> in Hunan area

Well	Depth (m)	Methane (‰)	Ethane (‰)	Propane (‰)	Isobutane (‰)	N-butane (‰)	Isopentane (‰)	N-pentane (‰)
H10	1825–1831	-39.689	-27.151	-25.960	-25.671	-26.839	-24.828	-25.911
HX1	2286.2–2449	-39.695	-27.436	-27.755	-28.922	-28.617	-26.680	-27.541
H18	2634–2639.6	-39.081	-25.896	-25.490	-24.117	-25.090	-23.777	-25.181

**Table 3** Test results of apatite fission track samples

Depression	Well	Depth (m)	Layer	Measured value		Analog value	
				Age (Ma)	Length (m)	Age (Ma)	Length (m)
Huhehu	H1	1845.13–1853.7	K <sub>1n</sub> <sup>2</sup>	67.2 ± 5.6	9.8 ± 2.6	68.7	11.1 ± 2.1
Hulunhu	HC3	1817.49–1828.49		57.0 ± 3.5	9.5 ± 2.5	61.6	10.6 ± 2.2

## Simulation experiment of hydrocarbon generation kinetics

The generation of oil and gas from source rocks under geological conditions is a long and complex geological process. Since the time temperature compensation relationship was put forward, there have been many experimental methods to simulate the hydrocarbon generation process of source rock by rapid temperature rise. Among them, the kinetic parameters obtained from the pyrolysis experiment carried out according to the kinetic principle can be used to simulate the evolution of hydrocarbon generation under geological conditions. In order to understand the influence of hydrocarbon generation process of coal measure strata on the formation of condensate reservoir, coal rock in the depth of 2240.99 m and carbonaceous mudstone in the depth of 1552.26 m of H2 well in Huhehu depression were sampled, and the dynamic pyrolysis experiment was carried out with gold pipe system. The pyrolysis was carried out at three heating rates of 2 °C/h, 6 °C/h and 20 °C/h respectively, and the pyrolysis gas products, C<sub>6</sub>-14, and C<sub>14</sub>+ were measured quantitatively, and the experimental principle and method are shown in reference Zhang (2014).

## Apatite fission track analysis

The fragments produced by Uranium 238 fission in apatite will form fission tracks in apatite. With the increase of temperature in geological time, the track length decreases and the density decreases (Duddy and Green 2006; Dou et al.

2021). Within 1 ~ 100 mA, the annealing temperature of apatite fission track is 60 ~ 150 °C, which is just close to the oil generation window (60 ~ 130 °C), so it is widely used in the study of paleogeothermal field in the basin. In order to clarify the influence of paleogeothermal changes on the formation of condensate reservoirs, samples were taken from Huhehu and Hulunhu depressions, and apatite fission track test and analysis were carried out. The experimental principle and method are shown in references Cui et al. 2018 and Cui and Ren 2013, and the experimental analysis results are shown in Table 3.

## Results

### Characteristics of condensate reservoirs

The condensate reservoirs discovered in the Hailar Basin are distributed in the Huhehu and Hulunhu depressions, and the burial depth of the reservoirs is generally less than 2700 m. By counting the components of 8 gas samples (Table 4), it is found that hydrocarbon gases account for more than 92% of the total volume of natural gas, and the higher the carbon number, the lower the content. The content of CH<sub>4</sub> is between 65.088 and 82.004%, the content of C<sub>2</sub>H<sub>6</sub> is between 7.644 and 11.587%, the content of C<sub>3</sub>H<sub>8</sub> is between 5.089 and 11.291%, the content of iC<sub>4</sub>H<sub>10</sub> is between 1.150 and 3.197%, and the content of nC<sub>4</sub>H<sub>10</sub> is between 0.715%. The content of iC<sub>5</sub>H<sub>12</sub> is between 0.228 and 1.121%, and nC<sub>5</sub>H<sub>12</sub> is between 0.167 and 0.638%. Non-hydrocarbon gas

**Table 4** Characteristic table of condensate components in the Hailar Basin

Depression	Well	Depth (m)	Formation	CH <sub>4</sub> (%)	C <sub>2</sub> H <sub>6</sub> (%)	C <sub>3</sub> H <sub>8</sub> (%)	iC <sub>4</sub> H <sub>10</sub> (%)	nC <sub>4</sub> H <sub>10</sub> (%)	iC <sub>5</sub> H <sub>12</sub> (%)	nC <sub>5</sub> H <sub>12</sub> (%)	H <sub>2</sub> S (%)	He (%)	H <sub>2</sub> (%)	CO <sub>2</sub> (%)	O <sub>2</sub> (%)	N <sub>2</sub> (%)	Relative density without air	
Huhehu	H10	1825.0–1831.0	K1n <sub>2</sub>	82.004	7.644	5.272	1.150	1.087	0.276	0.167				0.54		1.8	0.7018	
		1882.0–1877.8	K1n <sub>2</sub>	77.769	8.261	6.784	2.207	1.831	0.747	0.360				1.224			0.7748	
	H10	1882.0–1936.0	K1n <sub>2</sub>	76.153	8.172	7.859	2.654	1.915	0.741	0.335				1.491			0.7425	
		2286.2–2449.0	K1n <sub>2</sub>	65.088	10.525	11.291	3.197	3.616	1.121	0.638			0.017	3.221			0.992	0.8997
	HX1	1963.8–1970.0	K1d <sub>1</sub>	75.892	9.509	8.243	1.474	2.081	0.495	0.361				0.340			1.525	0.7646
		1927.8–2046.8	K1n <sub>2</sub>	79.625	8.391	5.089	1.439	1.155	0.496	0.272				2.495			1.038	0.7297
Hulunhu	HC3	2634.0–2639.6	K1n <sub>2</sub>	74.543	10.278	5.187	1.243	1.391	0.452	0.393		0.033	0.035	5.409			1.039	0.7710
		2068.0–2094.0	K1n <sub>2</sub>	72.824	11.587	7.497	1.653	0.715	0.228	0.236				0.638			2.765	0.7572

accounts for 2.340 to 7.496% of the total volume, mainly N<sub>2</sub> and CO<sub>2</sub>. The N<sub>2</sub> content is between 0.992 and 2.765%, and the CO<sub>2</sub> content is between 0.340 and 5.409%. In addition, very low levels of He and H<sub>2</sub> were detected in the H<sub>18</sub> well samples. The natural gas components of the two depressions are similar, and both are typical wet gas (Shen 2010; Gao et al. 2017). The origin of natural gas can be judged by using the carbon isotope data of natural gas components. The carbon isotopes of methane, ethane, and propane in Huhehu depression are -39.695 ~ -39.081‰, 27.436 ~ -25.896‰, and -27.755 ~ -25.490‰ (see Table 4). They are coal-derived gas, oil-type gas, and mixed gas (Dai et al. 1992) (Fig. 3). According to the diagram of the relationship between methane isotope and composition of Dai et al. 1992, the natural gas in the Huhehu depression is located in the condensate oil-associated or coal-type gas area (Fig. 4).

The condensate oil in the Hailar Basin has the characteristics of low density, low viscosity, low sulfur content, high gas-oil ratio, and high saturated hydrocarbons. The crude oil has a density of 0.7047–0.8069 g/cm<sup>3</sup>, and a viscosity distribution of 0.42–1.98 mPa·s. No sulfur components have been detected in the crude oil from Well H10 in the Huhehu depression. The saturated hydrocarbon content of the Huhehu depression is 70.83%, while the saturated hydrocarbon content of the crude oil in the Hulunhu depression is 82.5–83.7%, with an average of 83.1% (Table 5). The condensate-gasoline ratio in Huhehu depression is between 1450 and 10389m<sup>3</sup>/m<sup>3</sup>. According to the classification standard for condensate content (SY/T6168-1995 gas reservoir classification), it belongs to medium–high condensate reservoirs.

According to statistics, the condensate reservoirs discovered in the world are mainly structural reservoirs (Yang and Zhu 2013; Wu et al. 2017), and the condensate reservoirs in the Hailar Basin are structural and lithological-structural reservoirs. In the gentle slope zone of the Huhehu depression, there are many fault blocks or broken nose traps formed

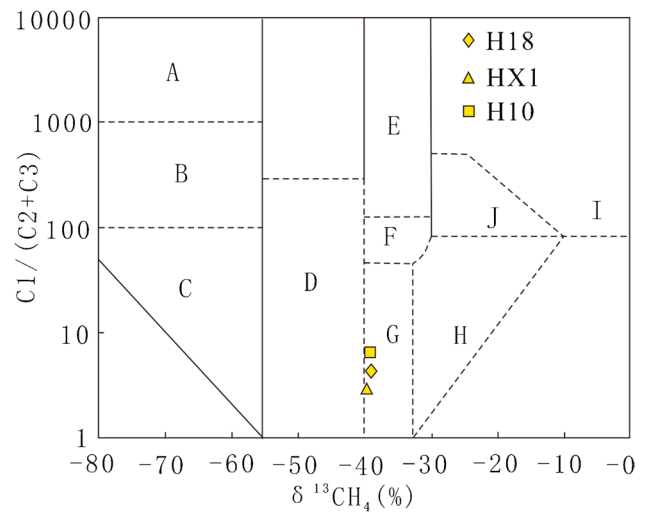


**Fig. 4** Graphic plate of methane isotope-composition relation of condensate gas in Huhehu depression. A: Biogas; B: Biological and sub-biogas; C: Sub-biogas; D: associated gas of crude oil; E: Oil-type cracking gas; F: oil-type cracking and coal-type gas; G: condensate associated and coal-type gas; H: coal gas; I: inorganic gas; J: Inorganic gas and coal gas

by north-east-trending reverse faults, and oil and gas accumulate in high positions of the traps (Fig. 5). Well H10 is located at the high part of the trap. Industrial oil and gas flows are obtained from the top of K<sub>1</sub>n<sup>2</sup>. The average porosity of reservoir is 14.9%, the permeability 4.52 × 10<sup>-3</sup> μm<sup>2</sup>. The oil reservoir area controlled by a single fault block in Well H10 is 3.3 km<sup>2</sup>, oil layer thickness is 23 m, and the oil column height is 120 m. Well HX1 is located in the lower part of the trap. During the drilling process, multiple oil and gas displays were seen. The span of the oil and gas displays is 420 m, but the burial is 350–600 m deeper than that of Well H10, which leads to poorer reservoir physical properties, with a porosity of 8.0% and a permeability of 0.1 mD, the oil test only obtains a small amount of oil flow, which

**Fig. 3** Carbon isotope identification plate of condensate gas in Huhehu depression. (Note: I- coal-derived gas province, II- oil type gas province, III- carbon isotope series inverted mixed gas province, IV-coal-derived gas and oil type gas province, V- coal-derived gas and oil type gas and mix gas province, VI- biogenic gas and the gas province)

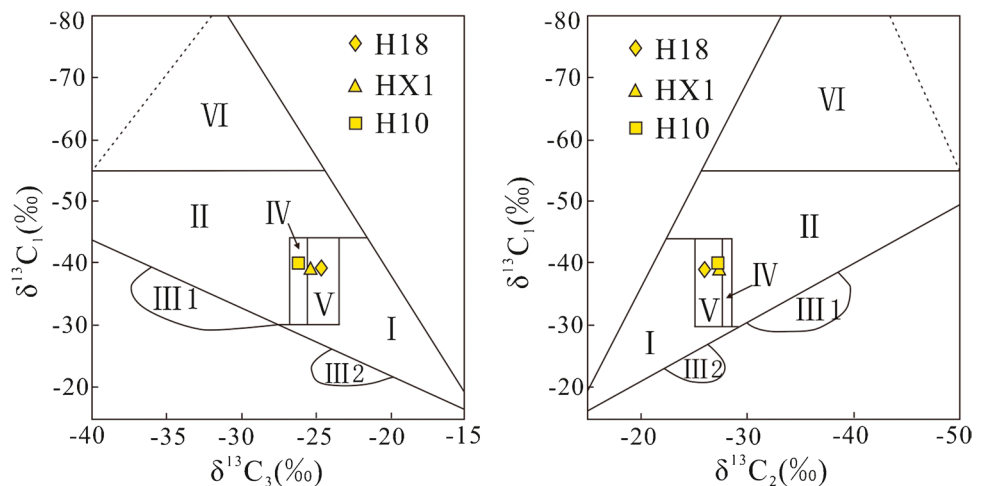


**Table 5** Characteristic table of condensate of petroleum components in the Hailar Basin

Depression	Well	Depth (m)	Formation	Relative density of oil	Viscosity mPa·s	Freezing point (°C)	Initial boiling point (°C)	Waxy (%)	Sulfur (%)	Asphaltene (%)	Colloid (%)	Carbon slag (%)	Ash (%)	Saturated hydrocarbon (%)	Aromatic hydrocarbon (%)	Non hydrocarbon (%)	Total hydrocarbon (%)
Huhehu	H10	1825.0–1831.0	K1n <sub>2</sub>	0.7047	0.42	-25	26		0.35					70.83	27.01	1.81	97.84
Hulunhu	HC3	2068.0–2094.0	K1n <sub>2</sub>	0.8069	1.98	-1	118	1.2	0.026	0.4	10	0.15	0.01	83.7	9.7	6.2	93.4
	HC3	2068.0–2094.0	K1n <sub>2</sub>	0.7988	1.62	4	110	2.3	0.029	0.9	7.6	0.19	0.05	82.5	9.4	7.2	91.9

has no industrial value. Therefore, with shallow burial and good reservoir physical properties, the area located in the high part of the trap is the favorable drilling position for obtaining industrial oil and gas flow.

### Accumulation mechanism of condensate reservoirs

According to the type of parent material, condensate oil can be divided into three categories: condensate oil produced by marine sapropel organic matter, condensate oil produced by humic organic matter in coal-measure strata, and condensate oil produced by mixed continental organic matter (Chen et al. 1994). The condensate reservoirs in the Hailar Basin are produced by the organic matter of the humus in the coal measures. According to the phase change during the formation of condensate gas reservoirs, it can be divided into primary condensate gas reservoirs and secondary condensate gas reservoirs. Primary condensate gas reservoirs are formed by gas generated from source rocks and directly migrated into traps in the gas phase, while secondary condensate gas reservoirs are often natural gas that has been cracked at high temperature during the thermal evolution of primary reservoirs. The formation of oil and gas reservoirs (Li 1998).

The thermal evolution of the source rocks of the coal measures in K<sub>1</sub>n<sup>2</sup> of the Hailar Basin is in the low-mature stage, with Ro in some of source rock greater than 1.3%. According to the saturated hydrocarbon chromatographic mass spectrometry analysis of crude oil and source rock, biomarkers such as sterane and terpane are the most effective microscopic parameters for oil source comparison. Saturated hydrocarbon chromatographic mass spectrometry analysis of crude oil from Well H10 in Huhehu depression and mudstone as well as coal of K<sub>1</sub>n<sup>2</sup> showed that the chromatographic fingerprint characteristics of the three were similar (Fig. 6), indicating that the oil and gas came from the coal-measure source rock of K<sub>1</sub>n<sup>2</sup>. It can be seen from the spectrum of terpenes (m/z = 191) that the C<sub>30</sub> content of the three is the highest, the content of gammacerane and tricyclic terpenes is very low, and the T<sub>m</sub> is higher than T<sub>s</sub>, both of which show low maturity. Features, it can be seen from the spectrum of sterane (m/z = 217) that the peak of C<sub>29</sub> sterane is higher than the peaks of C<sub>27</sub> and C<sub>28</sub> sterane, and the three spectral peaks are in the reverse “L” shape, which is typical of coal-derived oil and gas.

From the comparison of saturated hydrocarbon and aromatic hydrocarbon isotope oil sources, it is shown that the saturated hydrocarbon carbon isotope values of the crude oil in K<sub>1</sub>n<sup>2</sup> of the South Huhehu depression are between -24 and -29‰, and the aromatic hydrocarbon carbon isotope values are between -24 and -27‰. The isotopic characteristics of coal and mudstone in the section are similar (Fig. 7). The carbon isotope values of saturated hydrocarbons in the K<sub>1</sub>n<sup>1</sup> of mudstone range from -26.8 to -28.4‰, and



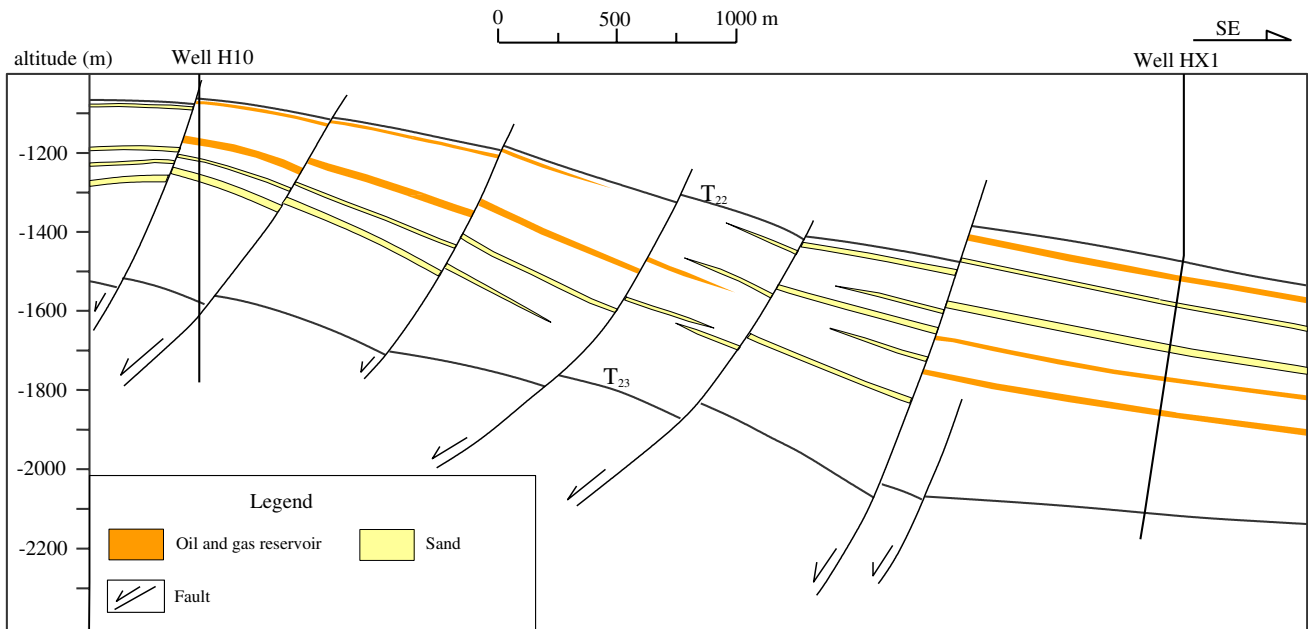
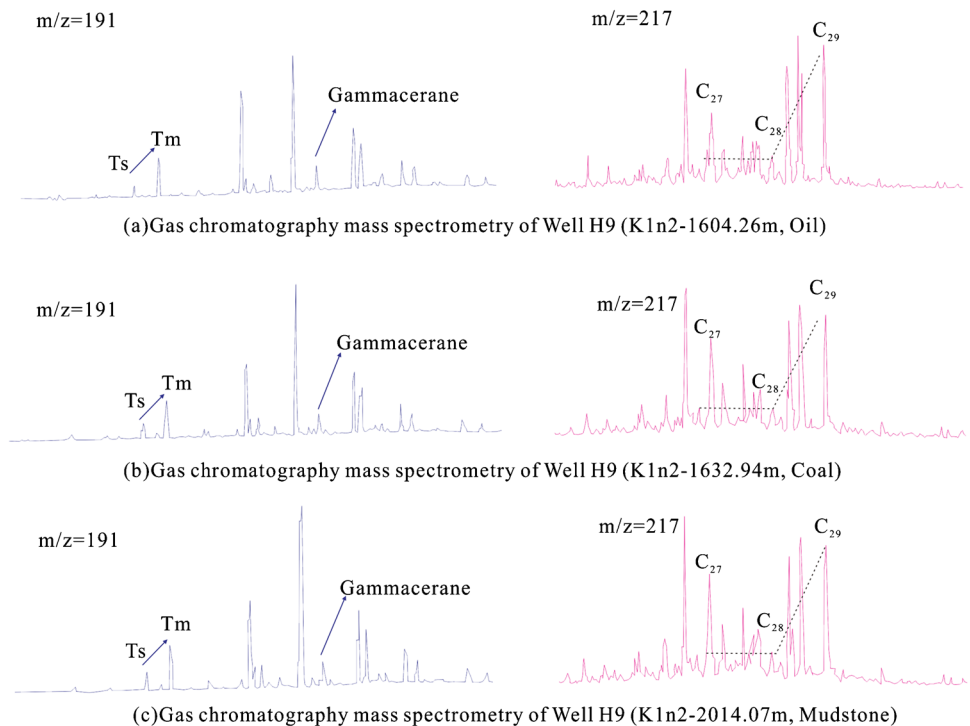


**Fig. 5** Oil and gas reservoir profile of well H10~HX1 in Huhehu depression

**Fig. 6** Comparison of GC–MS characteristics of saturated hydrocarbons between oil and source rocks in  $K_1n^2$  of Huhehu depression



the carbon isotope values of aromatic hydrocarbons range from  $-22$  to  $-24.5\%$ , which are obviously different from the crude oil isotope characteristics of  $K_1n$ . The generated oil and gas directly accumulate in the sandstone reservoirs of  $K_1n^2$ . The crude oil and the source rock have the same maturity and belong to the primary condensate reservoir.

The original gas-oil ratio and the composition of hydrocarbons are decisive factors affecting the phase state of hydrocarbon (Ding et al. 2018; Bao et al. 2018). Only when the formation temperature and pressure reach the critical value of the phase transition of hydrocarbons can condensate gas reservoirs be formed (Zhang et al. 2016). Appropriate

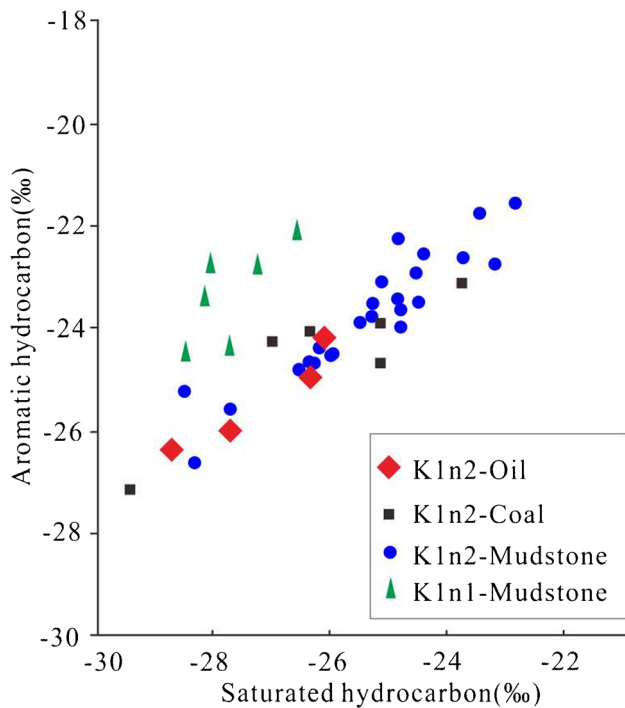


**Fig. 7** Oil source comparison chart of saturated hydrocarbon and aromatic hydrocarbon isotopic in Huhehu depression

temperature and pressure conditions and the coupling of temperature and pressure fields determine the formation and preservation of condensate gas reservoirs (Jiang et al. 2016). The special hydrocarbon generation conditions and temperature and pressure environment of the coal measures in the Hailar Basin have contributed to the formation of condensate oil and gas.

First, the characteristics of “early generation and early discharge, continuous gas generating” of coal is the prerequisite for the forming of condensate reservoirs. The gas content in hydrocarbons far exceeds that of liquids is the primary condition for the formation of condensate reservoirs (Tissot and Wehe 1984; Danesh 1998). At different stages of maturity, the production of condensate is the characteristic of coal-measure hydrocarbon generation (Sun et al. 2013; Li et al. 2016; Guo and Zhang 2017; Liu et al. 2017), and the generated hydrocarbons are dominated by gaseous hydrocarbons (Du 2005; Bao et al. 2017). Zhang (2014) carried out a high-temperature autoclave thermal simulation hydrocarbon generation experiment on the coal measure source rocks in the Huhehu Depression, and the results showed that both coal and mudstone are mainly gas generated, with very few liquid hydrocarbons (Zhang 2014). The total gas production of coal samples is 44.19 mg/g rock, the total oil discharge is 0.80 mg/g rock, and the total hydrocarbon production is 44.99 mg/g rock. However, the total gas production of coal measure mudstone is 0.90 mg/g rock, the oil discharge

is 0.21 mg/g rock, and the total hydrocarbon production is 1.11 mg/g rock. The oil discharge per unit of coal is 4 times that of mudstone, and the gas generation is more than 40 times that of mudstone. It shows that the hydrocarbon generation per unit of coal seam is much greater than that of coal measure mudstone.

According to the drilling statistics of 20 wells in the Huhehu depression, the thickness of the carbonaceous mudstone in  $K_{1n}^2$  of the South Huhehu depression is 59–475 m, and the thickness of the coal rock is 15–143 m. Indicating that the natural gas in this area is mainly generated from coal-measure source rocks. According to the study by Lu (1992), the threshold depth of coal kerogen gas formation in  $K_{1n}^2$  of the South Huhehu depression is about 900 m (Lu et al. 1993) (corresponding  $R_o$  is about 0.5%), and the initial point of obvious cracking into gas is 1700 m. That is to say, only small amount of liquid hydrocarbons generated from kerogen in coal measure source rocks begin to crack after the buried depth exceeds 1700 m (Lu 1996). When the buried depth reaches 2500 m, the generated liquid hydrocarbons begin to crack into gas in large quantities. Therefore, the coal rocks in the Huhehu depression show the characteristics of “early hydrocarbon generation and going on for long time, mainly gas generation.”

In this study, the experiment of hydrocarbon generation kinetics was carried out by sampling coal rock and carbonaceous mudstone in the Huhehu Depression. It can be seen that the hydrocarbon generation activation energy of source rocks is distributed between 36 and 74 kCal/mol, indicating a wide range of organic matter hydrocarbon generation (Fig. 8). Part of the activation energy is greater than 60 kCal/mol, indicating that the hydrocarbon generation potential can be continuously released after entering the mature stage. At the same time, there is also low activation energy of 36–52 kCal/mol, indicating that hydrocarbons can be generated under low-mature conditions.

By establishing and calibrating the dynamic models of oil, gas and oil pyrolysis gas generation, combined with the thermal history experienced by the source rock, the generation process of oil and gas can be quantitatively evaluated from the perspective of chemical kinetics, so as to obtain the hydrocarbon generation history of the source rock (Dong et al. 2011). It can be seen from the hydrocarbon generation and expulsion model diagram of coal rock (Fig. 9) that the liquid hydrocarbon production rate of coal rock is low, and the generated and discharged hydrocarbons are mainly gaseous hydrocarbons. When  $T_{max}$  is 445 °C and  $R_o$  reaches 0.73%, a large number of hydrocarbon begin to generation and discharge. Research on hydrocarbon generation history shows that the peak of hydrocarbon generation in the Huhehu depression is between 110 and 125 Ma (Fig. 10), indicating that a large amount of hydrocarbon began generating in the early coal measures of the Yimin Formation

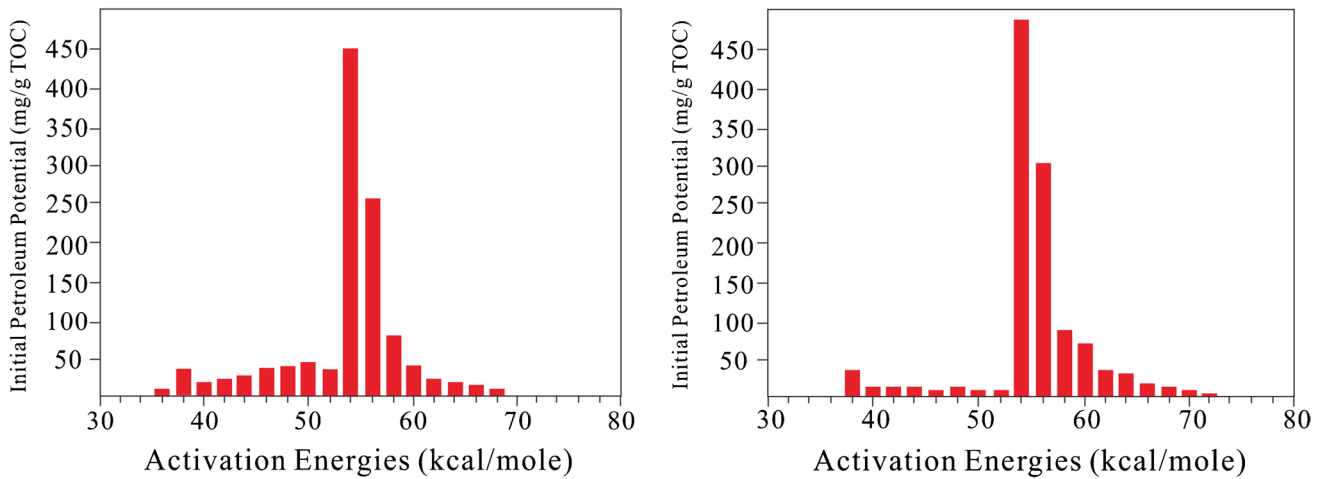


**Fig. 8** Activation energy distribution map of 2240.99 m coal rock (left) and 1552.26 m carbonaceous mudstone (right) in  $K_1n^2$  of He2 well in Huhehu depression

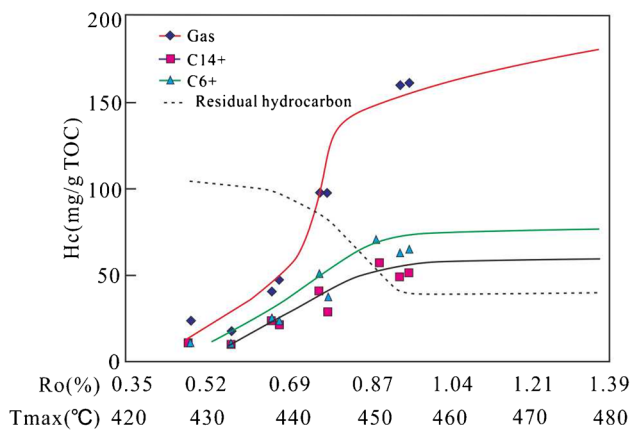
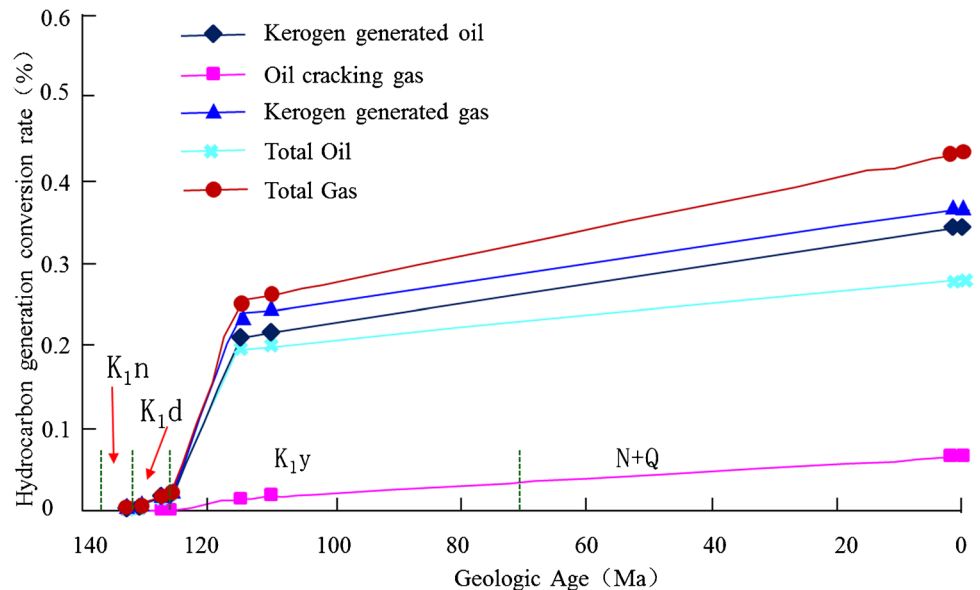


**Fig. 9** Hydrocarbon generation and expulsion pattern of coal and rock in Huhehu depression (data from Dong et al. 2011)

( $K_1y$ ), and it continued to this day. The humic kerogen of the coal measures in the Hailar Basin is dominated by gaseous hydrocarbons during the hydrocarbon generation process, forming a high original gas-oil ratio. Therefore, condensate oil and gas can be formed in the low-mature stage ( $R_o$  is 0.5–0.7%) system.

According to research on fluid inclusions captured in the Sulige gas field, coal produces different types of gas at various mature evolution stages (Lan et al. 2007; Zhang et al. 2009). Before  $R_o$  is less than 0.8%, the  $CO_2$  content is higher, but when  $R_o$  reaches 0.8–1.1%, the highly saturated hydrocarbon of  $C_{2+}$  produced by coal account, and when  $R_o$  is 1.4%, the amount of  $CH_4$  produced increases rapidly. The relative density of condensate gas that does not contain  $CO_2$  and  $N_2$  is relatively small. For example, the relative density of natural gas in most condensate gas

**Fig. 10** Hydrocarbon generation history curve of source rocks in Huhehu depression (data from Dong et al. 2011)



fields in the Tarim Basin is relatively low (0.621–0.655), and is dominated by secondary condensate reservoirs. Condensate gas in the Hailar Basin generally contains small amount of CO<sub>2</sub>, indicating that the CO<sub>2</sub> gas and hydrocarbon gas generated during the low-maturity period have entered the reservoir, further supporting the existence of primary oil and gas reservoirs.

Second, a stable temperature and pressure system is the guarantee for the formation of condensate reservoirs. Only when the formation temperature is between the critical temperature and the critical condensation temperature of the hydrocarbon system, and the original formation pressure is higher than the dew point pressure at this temperature, condensate reservoir will be formed (Wu et al. 2007). According to the research of Lu (1996), the Hailar Basin suffered uplift and denudation at the end of Nantun Formation and the end of Yimin Formation, and the amount of uplift and the largest denudation was at the end of Yimin Formation, reaching 500–700 m (Lu 1996).

According to the study of ancient geothermal temperature, the Yimin Formation was deposited in a cooling process (Cui and Ren 2013). The apatite fission track test and analysis were carried out by sampling the Huhehu and Hulunhu depression. The results are shown in Table 6. The maximum paleo-burial depth of the basin is the end of the Yimin Formation, which is also the most important accumulation period. The ancient geothermal gradient in Huhehu depression is 4.20 °C/100 m, the current geothermal gradient is 3.54 °C/100 m, and the ancient geothermal gradient in Hulunhu depression is 4.05 °C/100 m, the current geothermal gradient is 3.20 °C/100 m, both of which show that the current geothermal temperature is lower than that of the ancient geothermal. From the PVT phase diagram of the condensate gas reservoir of Well H10 in Huhehu Sag (Fig. 11), the formation temperature of the condensate gas reservoir is 68.75 °C, the temperature of the critical point K is 63.28 °C, and the critical condensate temperature K1 is 124.1 °C.

According to the thermal history model of apatite fission track restoration in the Huhehu depression (Fig. 12), during

**Table 6** Statistical table of measured formation pressure in Nantun Formation in Huhehu depression

Well	Formation	Depth (m)	Pressure (MPa)	Pressure coefficient
HC7	K1n2	1488.55	12.40	0.85
H2	K1n1	1645.50	10.87	0.67
H1	K1n2	1646.80	14.10	0.87
H6	K1n2	1664.70	13.82	0.85
H5	K1n2	2072.69	18.57	0.91
H8	K1n2	2317.50	17.82	0.78
H8	K1n2	2528.27	17.40	0.70

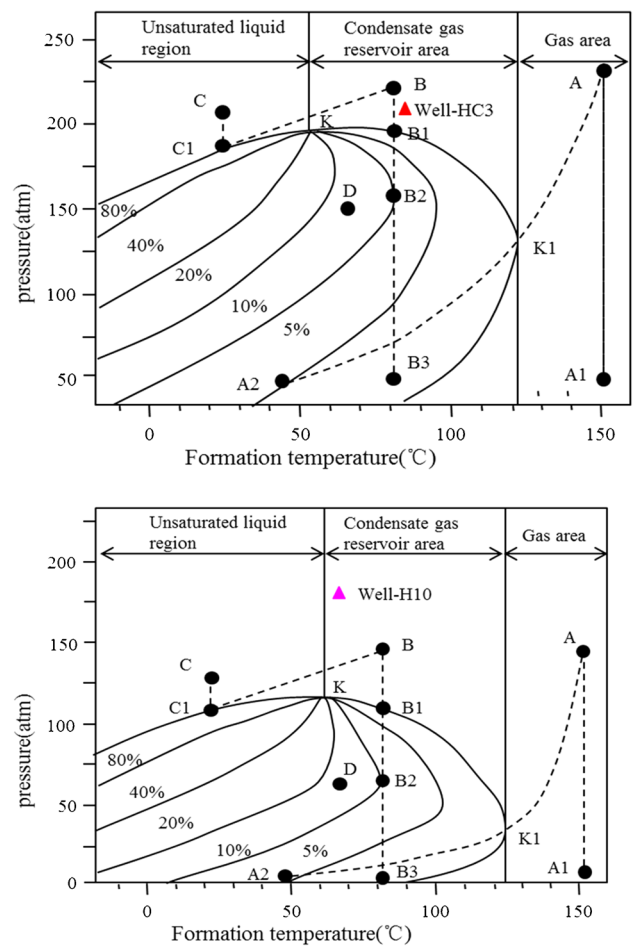
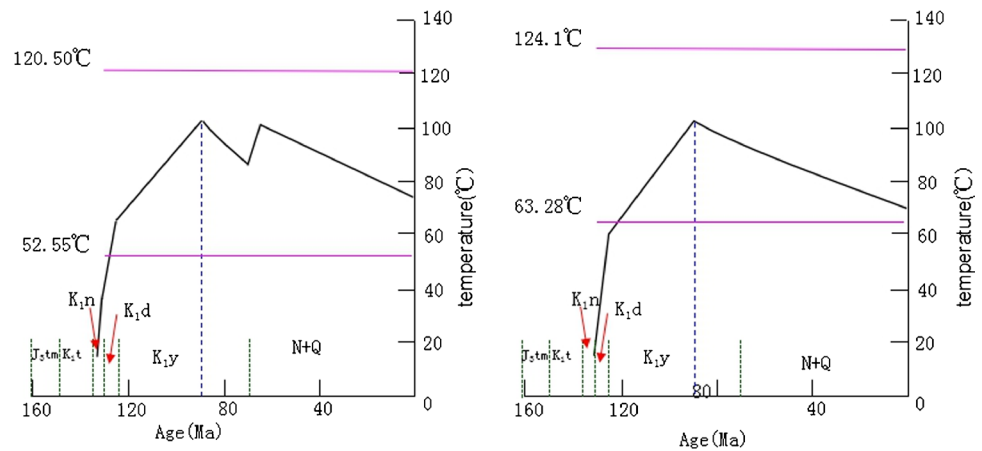


**Fig. 11** PVT phase diagram of condensate reservoir in well HC 3 (up) of Hulunhu depression and Well H10 (down) of Huhehu depression

the deposition period of the Damoguaihe formation, the formation temperature has reached above 60 °C and continued to rise, and the temperature at the end of the Yimin Formation was the highest, reaching 105 °C, the source rock can continuously generate hydrocarbons. The Huhehu depression has been buried and heating up until 90 Ma (the end of Yimin Formation), and then cooling down after Yimin formation, but the formation temperature has always been between the critical point temperature of 63.28 °C and the critical condensate temperature of 124.10 °C, which is conducive to the formation of condensate oil and gas. From the PVT phase diagram of the condensate gas reservoir of Well HC3 in Hulunhu depression (Fig. 11), the formation temperature (83.0 °C) of Well HC3 is between the critical point temperature (K = 52.55 °C) and the critical condensate temperature (K1 = 120.50 °C), which just distributed in the condensate gas reservoir area. From the thermal history model of the apatite fission track recovery in Well HC3 (Fig. 12), it can be found that there was one heating process until 90 Ma (the end of the Yimin Formation), followed by two cooling

**Fig. 12** Thermal history model of apatite fission track recovery in well HC3 of Hulunhu depression (left) and well H10 of Huhehu depression (right)



process, but the formation temperature has been at the critical point of 52.55 °C and the critical condensate temperature of 120.50 °C, indicating that the formation temperature from the end of the Damoguaihe Formation is favorable for the formation of condensate oil and gas.

In the K1d1 of Huhehu and Hulunhu depression, mudstone layers are developed with a thickness of 500–1000 m, which can effectively prevent the upward loss of oil and gas and form a good regional caprock. According to the statistics of 7 measured data from 6 wells, the formation pressure coefficient of Nantun formation in Huhehu depression is 0.67–0.91, with an average of 0.81 (Table 6), which belongs to low abnormal formation pressure. In addition to under compaction, the formation pressure will also decrease with the decrease of formation temperature (Xu et al. 2009; Zhao et al. 2017), and the cooling process after the deposition of the Yimin Formation will also promote the formation of abnormal low pressure in  $K_{1n}^2$ . The emergence of abnormal low pressure reduces the dissolution of gaseous hydrocarbons in liquid hydrocarbon (Wang et al. 2015), which is more prone to reverse evaporation than formations under normal pressure systems or high abnormal pressure systems, and higher gasoline ratios are likely to form condensate oil and gas.

### Main controlling factors of condensate oil and gas accumulation

The coal-measure strata in  $K_{1n}^2$  have the characteristics of “integrated source and reservoir.” The oil and gas generated from the coal-measure source rocks can migrate into the sand body at a short distance, forming a self-generating and storing source-reservoir-cap combination.

First, the effective hydrocarbon expulsion range controls the horizontal distribution of oil and gas. From the above hydrocarbon generation simulation experiment analysis of coal rock and mudstone, it can be found that the oil

generation and drainage volume of coal rock is greater than that of coal measure mudstone. According to the simulation results of hydrocarbon generation and expulsion of unit mass coal and mudstone, the hydrocarbon expulsion intensity of coal and mudstone at the well point can be calculated. Combined with the plane prediction of thickness and maturity of coal and mudstone, the isoline distribution of oil expulsion and exhaust intensity of coal and mudstone on the plane can be obtained.

From the graphs of coal and mudstone oil and gas discharge intensity (Fig. 13 and Fig. 14), it is clear that the south is higher than the north, and most of the wells that obtain oil flow or oil and gas shows are located in effective source rocks. In the hydrocarbon range, most wells far away from the hydrocarbon expulsion range have no oil and gas shows. The area with the highest value of coal and rock oil discharge intensity on the plane is located between wells HC1-H7 in the south, with the highest value being  $0.6 \times 10^6$  t/km<sup>2</sup>, and generally  $0.1\text{--}0.5 \times 10^6$  t/km<sup>2</sup>. The highest in the north is  $0.3 \times 10^6$  t/km<sup>2</sup>, and the south is higher than the north (Fig. 13). Areas with high exhaust intensity are also mainly distributed in the south, up to  $50 \times 10^8$  m<sup>3</sup>/km<sup>2</sup>, located near wells H8 and H7, generally  $5\text{--}30 \times 10^8$  m<sup>3</sup>/km<sup>2</sup>, and the highest in the north is  $25 \times 10^8$  m<sup>3</sup>/km<sup>2</sup>, greater than  $10 \times 10^8$  m<sup>3</sup>/the area of km<sup>2</sup> is located between Well H5 and Well H1. Oil and gas discharge intensity of mudstone are obviously lower than that of coal rock. The maximum oil discharge intensity is located near Well HX1 in the south, with a value of  $0.06 \times 10^6$  t/km<sup>2</sup>, generally  $0.02\text{--}0.04 \times 10^6$  t/km<sup>2</sup> (Fig. 14). The maximum mudstone exhaust intensity is located between the HX1 and H8 wells, with a value of  $30 \times 10^8$  m<sup>3</sup>/km<sup>2</sup>, generally  $5\text{--}20 \times 10^8$  m<sup>3</sup>/km<sup>2</sup>, and the maximum value in the north is  $10 \times 10^8$  m<sup>3</sup>/km<sup>2</sup>. Drilling well revealed that the effective source area and thickness of the southern sag of the Huhehu depression are larger than those of the northern sag, and the exploration effect is also better than that of the Hubei sag, further confirming that the

**Fig. 13** Oil expulsion intensity (up) and gas expulsion intensity (down) of coal in Huhehu depression

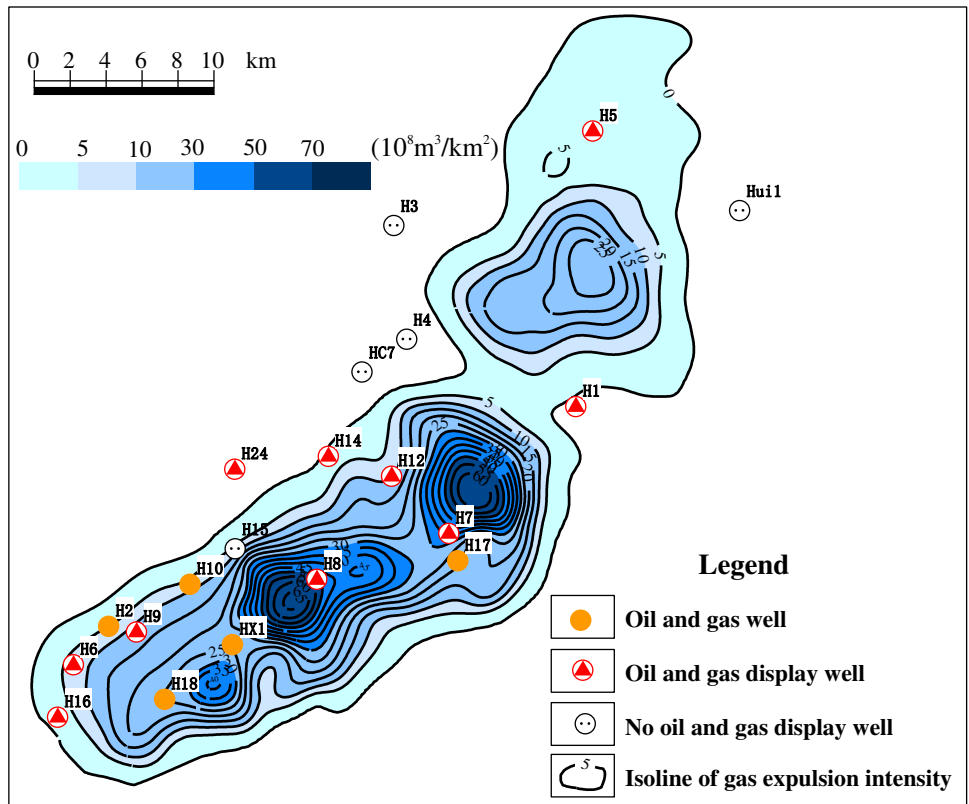
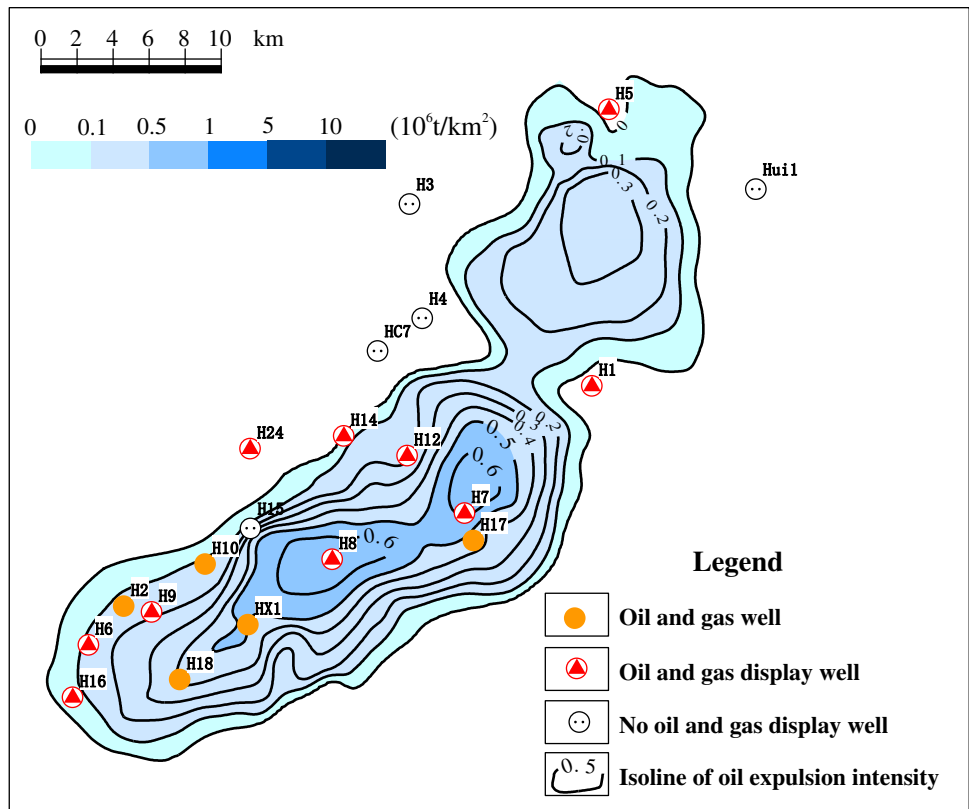
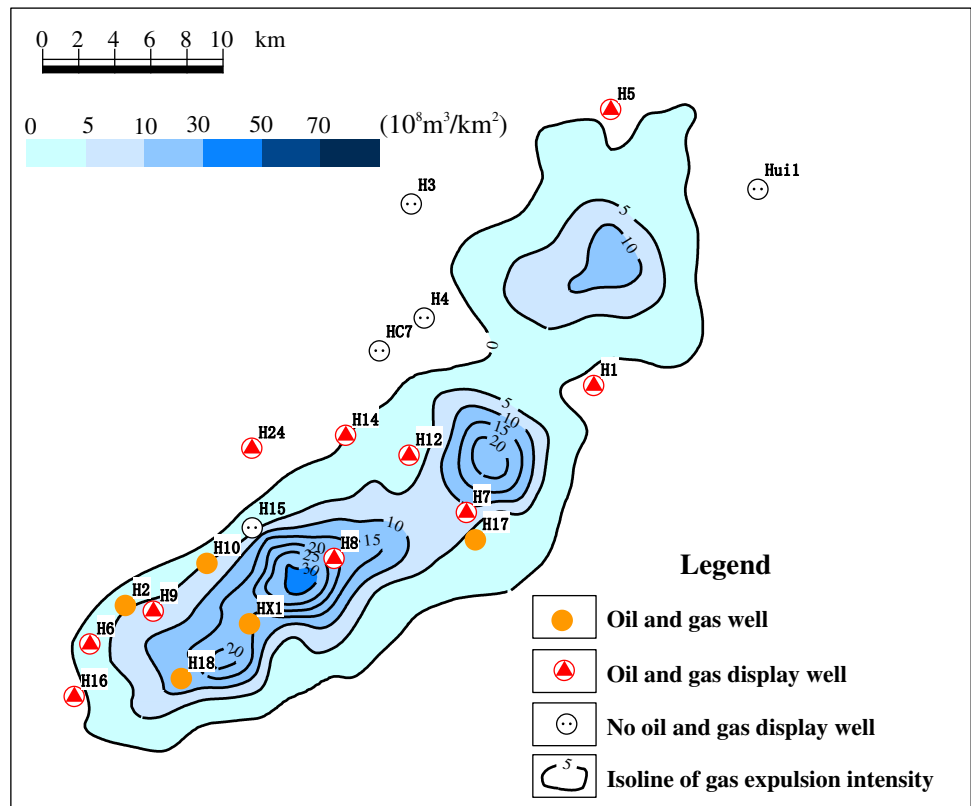
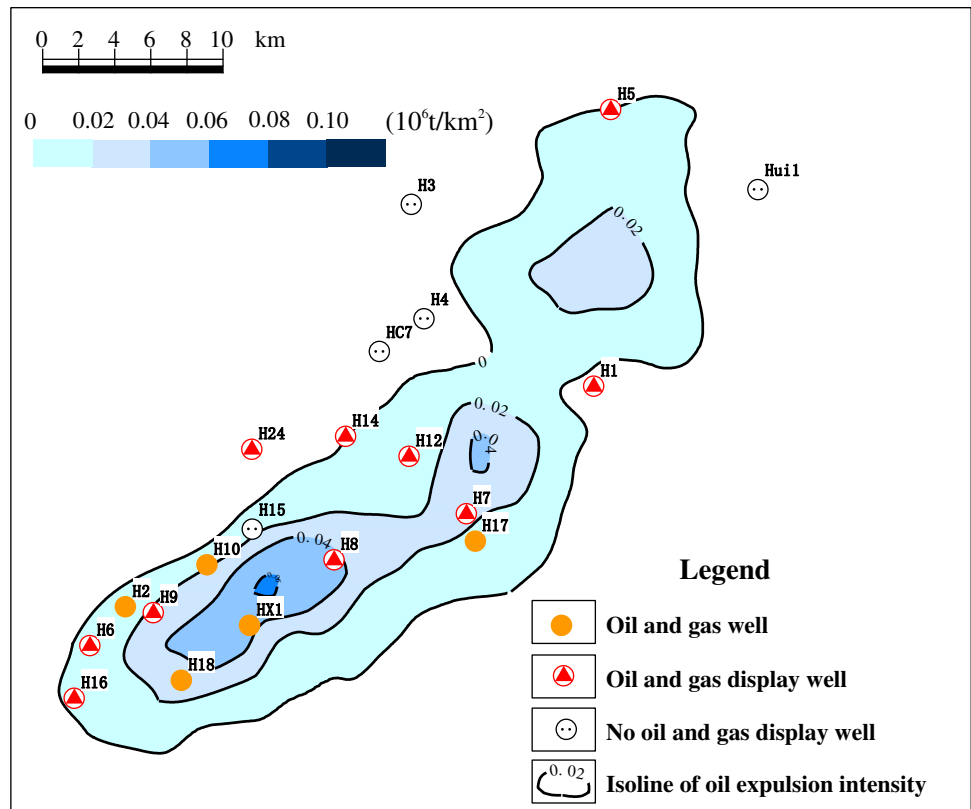


**Fig. 14** Oil expulsion intensity (up) and gas expulsion intensity (down) of mud stone in Huhehu depression



effective hydrocarbon expulsion range of the hydrocarbon-generating depression controls the horizontal distribution of oil and gas.

Second, sand bodies, faults, and unconformities control the direction of hydrocarbon migration. The transport system for oil and gas migration in the coal-measure strata of  $K_1n^2$  of the Hailar Basin is composed of sand bodies, faults, and unconformities. Due to the small scale, thin thickness, and poor lateral connectivity of single sand bodies during the rifting-depression period, it is difficult for oil and gas to move along the heights. Porous and permeable sand bodies undergo large-scale and long-distance migration, mainly in vertical migration and short-distance lateral migration (Fig. 15). Long-term active faults control the direction of oil and gas migration (Jia et al. 2017). Not only can faults themselves become good channels for oil and gas migration, but also faults can communicate up and down unconformities or sand bodies, so that oil and gas migrate in a “step-like” manner. According to statistics of 15 wells in the Huhehu and Hulunhu depression, it is found that oil and gas are basically enriched near the unconformity surface of T22, and most of the oil and gas shows are concentrated within 300 m from the top.

(profile location seen from Fig. 1).

Third, regional caprock controls vertical hydrocarbon enrichment horizons. Good preservation conditions are the prerequisite for the formation of oil and gas reservoirs (Guo et al. 2010), and the formation of large-scale natural gas fields is controlled by the regionally stable distribution of abnormally high pressure mudstones (Osborne and

Swarbrick 1997; Douglas 2001; Broichhausen et al. 2005; Xue and Li 2018). The high-quality caprock has abnormal pore fluid pressure, which can effectively prevent the vertical escape of condensate gas, maintain a certain oil–gas ratio and a stable critical condensate temperature and pressure system. For example, the gypsum-salt layer of the lower part of the fourth member of the Shahejie Formation in the Dongying Sag of the Bohai Bay Basin in eastern China (Wang 2007; Yang and Zhu 2013), the huge thick gypsum-salt rock of the Jidike formation of the Neogene in the Kuqa Depression in the west, the mudstone of the Sangtam Formation in the central Tarim Basin, and the Lianglitage Group marls play an important role in the preservation of condensate reservoirs. The thick mudstone of  $K_1d^1$  is a good regional caprock for the oil and gas reservoir of  $K_1n^2$ . The Hailar Basin has developed two-stage fault systems. The fault systems formed during the rifting period are mainly developed in  $K_1n^2$  and below, and the fault systems formed during the rifting-depression period are mainly developed in  $K_1n^2$  and above, most of which disappear at the top of  $K_1d^1$  (Fig. 15). Good caprocks in  $K_1d^1$  can effectively prevent oil and gas from dissipating upward, and oil and gas are mainly distributed in  $K_1n^2$ .

### Condensate hydrocarbon accumulation models

The matching of structures and high-quality reservoirs controls the formation of oil and gas reservoirs. Oil and gas

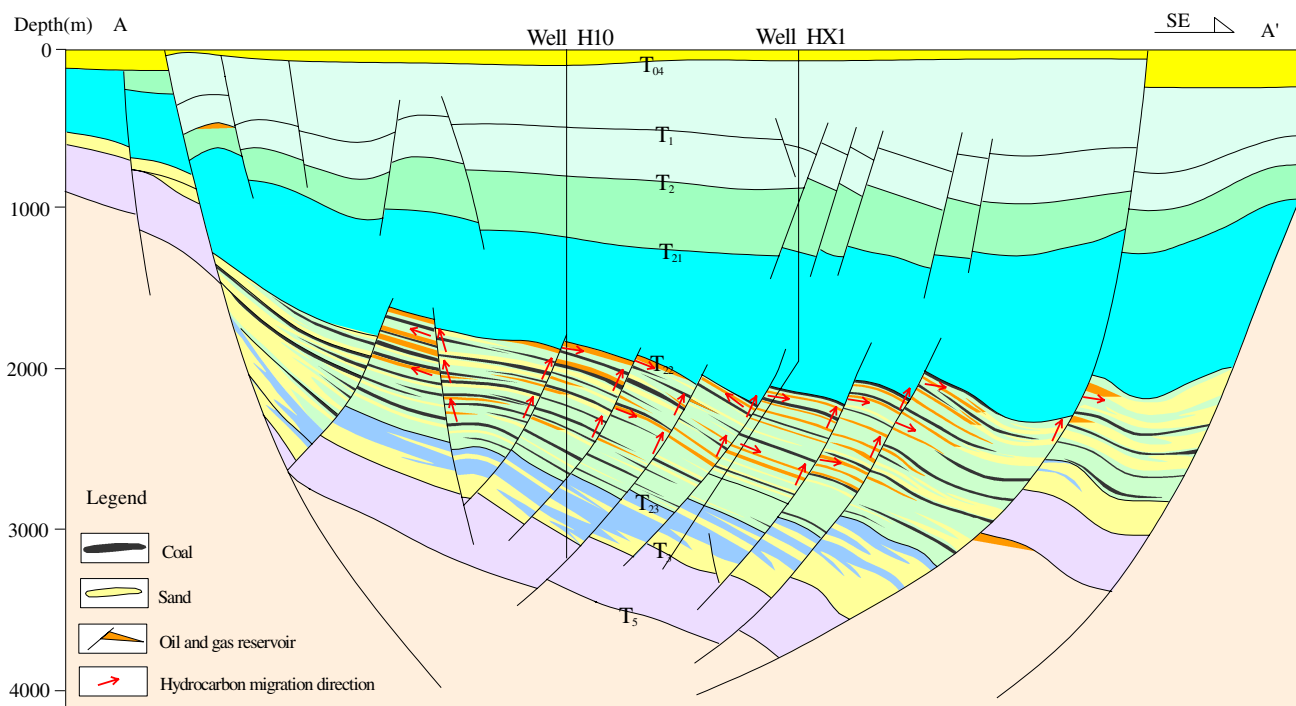


**Fig. 15** Hydrocarbon accumulation map of Huhehu depression, southern Hailar Basin



mainly accumulate in structural traps that are well matched to effective reservoirs. The structural high points are the richest, and they are distributed in steep and gentle slope zones.

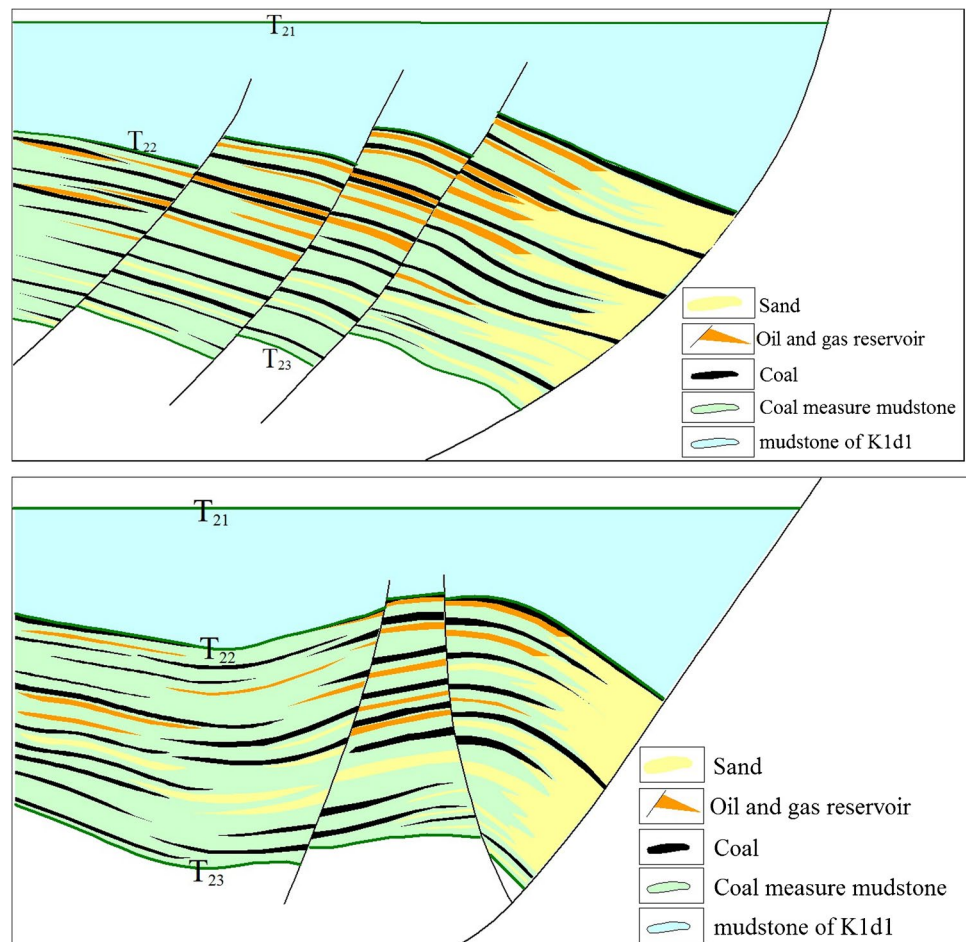
The steep slope zone of  $K_1n^2$  is generally a multi-level fault stage composed of depression-controlling faults and associated secondary faults. By the control of the structural background, fault noses and fault block traps are distributed in the high part of the fault stage. The fan delta front sandbodies controlled by syn-sedimentary faults in the lower part of the fault step are pinched in the updip direction near the depression area, and the lateral direction is blocked by the fault, forming a fault-lithological trap. The steep slope zone develops two accumulation modes of fault step and anticline types.

The fault-step steep slope zone formed by the main control fault and the secondary fault is characterized by the development of multi-level reverse fault steps. The first section of the main control fault forms multiple sub lacustrine fans at the root of the main control fault, distributed in the dark mudstone, and formed by the fault cutting, source-up-reservoir fault-lithologic oil and gas reservoirs, due to the interaction of fan delta sand bodies with mudstone and coal

seams in  $K_1n^2$ , matching with the reverse faults, self-generating and self-reserving fault blocks and fault-lithologic oil and gas reservoirs (Fig. 16). The typical well is H1, located within the effective source rock range, with the coal thickness of 23.6 m, mudstone thickness of 75 m, and sandstone thickness of 29.4 m, located in the lower part of the reverse fault block, with large fault distance (55 m), multi-layer oil-bearing, low-yield oil flow obtained, and structural oil reservoirs developed. The southern sag of the Huhehu depression, the northern sag of the Hulunhu depression, and the northern sag of the Yimin depression all develop fault-step-type steep slope belts, which are favorable areas for the exploration of condensate reservoirs.

Large-scale rolling anticlines develop under the main control fault activity and are complicated by secondary faults. The oil and gas generated from the coal measure strata in  $K_1n^2$  directly enters the adjacent sand bodies and accumulates in the high part of the trap to form faulted anticline oil and gas reservoirs (Fig. 16). The H17 well area in the Huhehu depression is a typical anticline condensate reservoir. Well H17 is located in the effective source rock range, with coal of 10.6 m, mudstone of 63 m, sandstone thickness of 30 m, and average porosity of 15.3%. It located in the high

**Fig. 16** Petroleum accumulation model map of Condensate Oil and Gas Reservoir of faulted terrace type (up) and anticline type (down) steep slope belt



part of the faulted anticline trap, and contains multiple layers of oil. The gas test yielded 14,036 cubic meters per day. Industrial gas flows and structural oil and gas reservoirs are developed. Fluorescent siltstone was seen in the low part of Well He7, with poor physical properties and 10.6% porosity. There are many rolling anticlines in the Huhehu, Hulunhu, and the steep slope belt of the Yimin depression. The accumulation conditions are superior, which is a favorable area for the next exploration.

The gentle slope zone has a controlled depression and fault tilting action, frequent structural activities, well-developed faults, and multiple fault steps. The upper fault step belt is dominated by forward faults, mainly developed fault blocks and fault nose structures, and the strata are overlaid and regressed. In the  $K_1d^2$  and Yimin formation, the oil and gas formed in the Nantun Formation migrated upward along the depression-controlling faults, forming secondary fault-block reservoirs locally. The lower fault step belt is dominated by reverse faults, with fault blocks and fault nose traps developed. During the deposition of the Nantun Formation, braided river delta and fan delta sand bodies were widely developed, and adjacent to hydrocarbon-generating depressions, they depended on sandbodies-fault-unconformity drainage system migrates in steps, controlled by faults and sub-faults in the controlled zone, forming structural, lithological-structural oil and gas reservoirs, and locally distributed sandstone updip pinching and fault-lithological oil and gas reservoirs (Fig. 17).

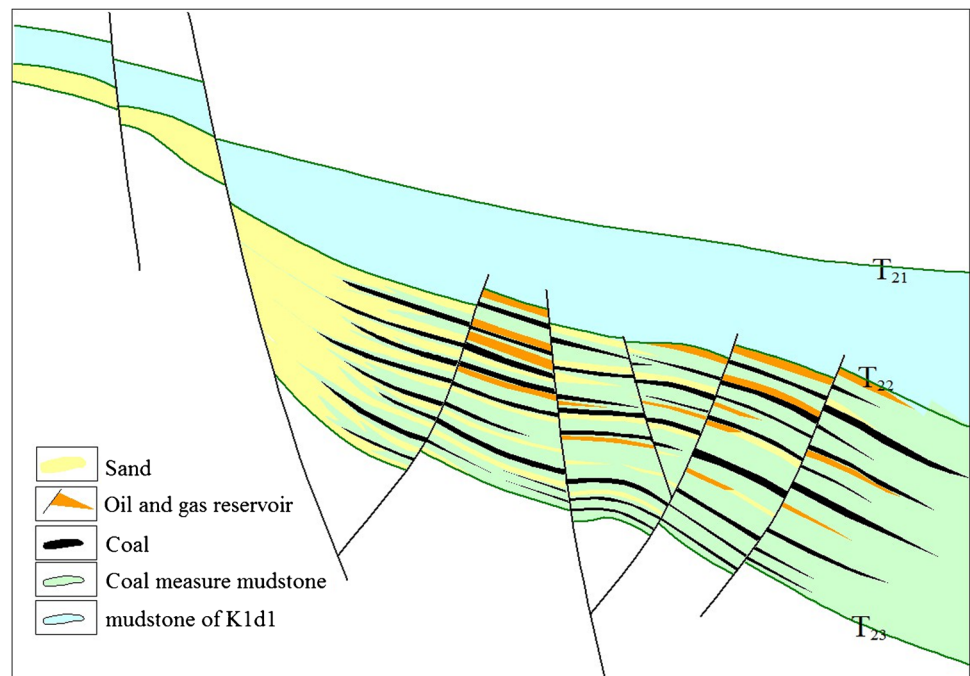
A typical condensate reservoir in the gentle slope zone is well H10 reservoir in Huhehu depression. Well H10 is located in the braided river delta plain subfacies, in the

center of hydrocarbon generation of coal and mudstone. The thickness of  $K_1n^{2-1}$  coal is 5.0 m, mudstone 80 m, and the channel sand body is well developed, which located in the effective reservoir development area, with the thickness of 36 m, porosity 16.8%. It is located in the high part of the reverse fault block, with good physical properties (average porosity 16.8%), small fault distance (15 m), multi-layered oil, and industrial oil and gas flow obtained, and structural oil reservoirs are developed. Therefore, oil and gas in the fault-step gentle slope zone are mainly enriched in reverse fault block traps that match the effective reservoir. The southern sag of the Huhehu depression, the northern sag of the Yimin depression, and the southern sag of the Chaganuoer depression have similar accumulation conditions and are key areas for further exploration.

## Discussion

Regarding the source of oil and gas, it has been discussed above that the condensate oil and gas in the Hailar Basin comes from the coal-measure source rock of  $K_1n^2$ , but whether it comes from coal or mudstone is still uncertain. Discuss whether the condensate oil and gas mainly come from coal or mudstone, which has important indicative significance for the next oil and gas exploration. If mudstone contributes a large amount of oil and gas sources, the next exploration should be carried out around the effective hydrocarbon expulsion range of mudstone. Conversely, if coal rock contributes significantly to the source of oil and gas, exploration should be done around the coal rock hydrocarbon

**Fig. 17** Petroleum accumulation model map of Condensate Oil and Gas Reservoir of gentle slope belt



expulsion center. From the comparison of saturated hydrocarbon and aromatic hydrocarbon isotope oil sources in the Huhehu depression, it can be found that the isotopes of coal and mudstone are distributed in the same area and cannot be separated. The organic matter types of coal in  $K_1n^2$  of the Hailar Basin are II2-III, which is similar to the mudstone organic matter. Kerogen is mainly hydrogen rich vitrinite, including sporophytes, liposomes, and other components, indicating that this area is dominated by higher plants, and the vitrinite is rich in hydrogen due to biochemical effects such as bacterial degradation in the later stage (Fig. 18).

Due to its complex composition and different microscopic components with different oil-generating thresholds, the hydrocarbon generation zone will cover a large area. Judging from the activation energy distribution obtained from this hydrocarbon generation kinetics experiment, both mudstone and coal have a wide distribution range of activation energy for hydrocarbon generation. The main activation energy distribution areas are 54–60 kCal/mol, indicating that mudstone and coal rock have similar hydrocarbon generation potential. The results of high-temperature and high-pressure thermal simulation experiments show that the gas generation volume per unit mass of coal rock is more than 40 times that of mudstone, and the exhaust gas volume is 4 times that of mudstone. From the perspective of the hydrocarbon generation process, a large amount of hydrocarbons have been generated and expelled from coal samples from 300 °C, and a large amount of hydrocarbon gas is still produced when heated to 500 °C, while mudstones begin to generate and expel a

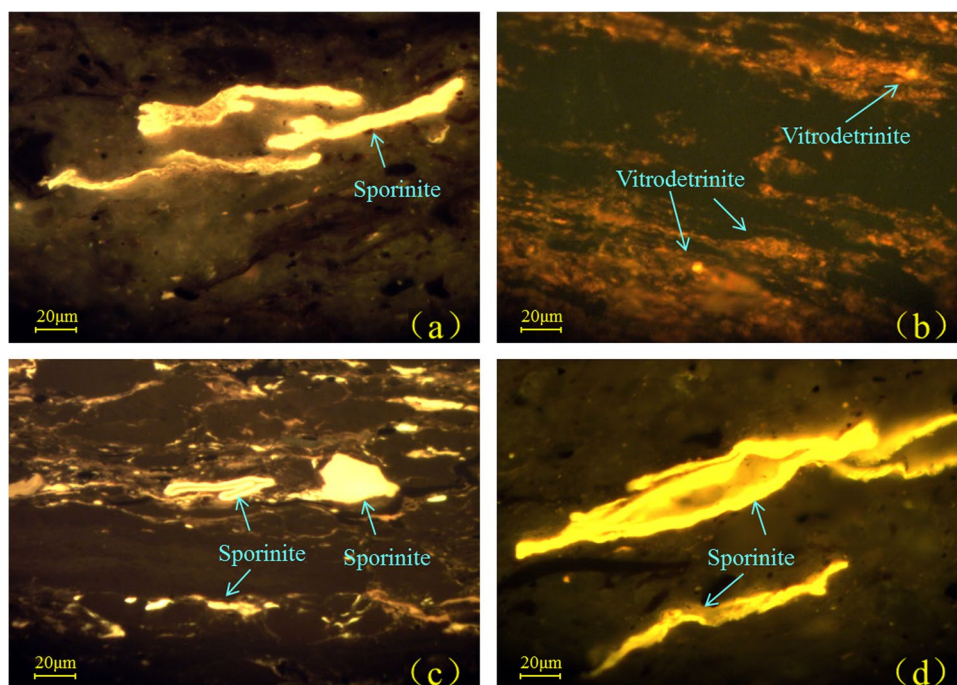
lot of hydrocarbons only after 350 °C, which shows that in the same geology conditions, the amount of oil and gas that can be generated and discharged per unit mass of coal is more than that of mudstone.

It is worth noting that in the underground formation, the oil and gas reservoir mainly exists in a single gas phase. When it is produced on the surface, it forms reverse condensate due to the change of temperature and pressure, which is also the reason why the condensate oil and gas production in Huhehu and Hulunhu depression is mainly condensate gas and less condensate oil. From the perspective of hydrocarbon expulsion intensity, coal is stronger than mudstone in terms of oil expulsion intensity, and has a wider distribution range. Therefore, exploration around the traps developed around the hydrocarbon expulsion center of coal is the first choice. Of course, the hydrocarbon expulsion centers of coal and mudstone in the Huhehu depression are basically the same. Mudstone can be used as a local caprock overlying oil and gas reservoirs, which is very beneficial to the preservation of oil and gas reservoirs.

## Conclusions

Condensate reservoir in the Hailar Basin is generated from humus organic matter in coal-measure strata. They have a high gas-oil ratio and belong to gas reservoirs containing medium–high condensate oil. According to phase changes during the formation of condensate gas reservoirs, they are primary condensate reservoirs.

**Fig. 18** Microscopic fluorescence photos of coal measures source rocks in  $K_1n^2$  of Hailar Basin. (a) H6 well, 1492.67 m, coal,  $\times 500$ ; (b) HX1 well, 3062.17 m, coal,  $\times 500$ ; (c) H9 well, 1635.94 m, mudstone,  $\times 500$ ; (d) H2 well, 1550.46 m, mudstone,  $\times 500$



The special hydrocarbon-generating conditions and geological environment of the coal-measure strata have contributed to the formation of condensate reservoirs: coal rocks are dominated by gas generation but very few oils, and have the characteristics of “early generation and discharge, continuous gas generating.” The sealing of big thickness mudstone of the  $K_1d^1$  to form a stable temperature and pressure system are the guarantee for the formation of condensate reservoirs.

The distribution range of effective source rocks controls the distributed areas of condensate hydrocarbon reservoirs. Sand bodies, faults, and unconformity surfaces control the direction of oil and gas migration, and the regional caprocks of  $K_1d^1$  control the vertical oil and gas enrichment horizons. The oil and gas are mainly distributed in the  $K_1n^2$  of the strata.

The coal-measure strata of  $K_1n^2$  have the characteristics of “integration of source and reservoir.” The matching of structure and reservoir physical properties controls the accumulation of condensate reservoirs, which distribute in the fault step steep slope zone, anticline steep slope and gentle slope fault terrace. The southern sag of Huhehu and Chaganuoer depression, northern sags of Hulunhu, and Yimin depression are the favorable exploration areas.

## Declarations

**Conflict of interest** The authors declare no competing interests.

## References

- Bao JP, Zhu CS, Shen X (2018) Study on diamondoids and genetic mechanism of condensates from the Kela 2 structure in the Kuche Depression. *Nat Gas Geosci* 29(9):1217–1229. <https://doi.org/10.11764/j.issn.1672-1926.2018.07.015> (in chinese)
- Bao SY, Zhang LY, Zhang SH, Wang YR, Zhang L, Wu LB, Miao CX, Zhang JG (2017) Simulation experiment and mechanism of hydrocarbon-generation retardation for source rocks. *Acta petrolei sinica* 38(7):753–762. <https://doi.org/10.7623/syxb201707003> (in chinese)
- Broichhausen H, Littke R, Hantschel T (2005) Mudstone compaction and its influence on overpressure generation, elucidated by a 3D case study in the North Sea. *Int J Earth Sci* 94(5–6):956–978. <https://doi.org/10.1007/s00531-005-0014-1>
- Cao YJ, Wang Q, Zou HY, Diao F, Lin JF, Zhang JF, Guo LX (2017) Genesis types and distribution laws of crude oil in Langgu sag. *ACTA PETROLEI SINICA* 38(11):1263–1274. <https://doi.org/10.7623/syxb201711005> (in chinese)
- Chen HP (2014) Geochemical characteristics of source rocks and oil source correlation of coal measures in Nantun Formation, Huhehu depression. *West-China Explor Eng* 1:50–54. <https://doi.org/10.3969/j.issn.1004-5716.2014.01.016> (in chinese)
- Chen H (2015) Geological conditions of forming condensate gas reservoir in southern Huhe lake depression, Hailar Basin. *Nat Gas Explor Dev* 38 (3): 7–11. <https://doi.org/CNKI:SUN:TRKT.0.2015-03-002>. (in chinese)
- Chen JL, Shen P, Wen QB (1994) The genetic type and geochemical characters and their significance of the condensates in China. *Acta Sedimentol Sin* 13(1):32–39. <https://doi.org/10.1007/BF02006258> (in chinese)
- Chen JL, Wu HY, Zhu DF, Ling CH, Yu DS (2007) Tectonic evolution of the Hailar Basin and its potentials of oil-gas exploration. *Chin J Geol* 42(1):147–159. <https://doi.org/10.3321/j.issn:0563-5020.2007.01.013> (in chinese)
- Cui JP, Ren ZL (2013) Research on the Paleotemperature in Hailaer Basin. *Geol Sci Technol Inf* 32 (4): 151–156. <https://doi.org/CNKI:SUN:DZKQ.0.2013-04-023>. (in chinese)
- Cui JP, Zhao J, Ren ZL, Jin W, Xin L, Wang YQ (2018) The geochemical characteristics of lower cretaceous source rocks and thermal history in the Huhehu Depression, Hailar Basin. *Earth Sci* 45(1):238–250. <https://doi.org/10.3799/dqkx.2018.300> (in chinese)
- Dai JX, Pei XG, Qi HF (1992) *Natureal Gas Geology in China*(vol.1). Beijing: Petroleum Industry Press: 65–87 (in chinese)
- Danesh A (1998) *PVT and Phase Behaviour Petroleum Reservoir Fluids*[M]. Amsterdam: Elsevier:108–113
- Ding WJ, Hou DJ, Chen L, Gan J, Liang G, Ma XX, Wu P, Wang H, Feng XQ (2018) Characteristics and origin analysis of a unique genetic type of natural gases in Songnan-Baodao sag, southeast Qiong basin. *J Northeast Pet Univ* 42(3):1–15. <https://doi.org/10.3969/j.issn.2095-4107.2018.03.001> (in chinese)
- Dong L, Wang WM, Yu XB, Wang GH (2011) Study on hydrocarbon accumulation stages in Nantun formation, Huhehu depression, Hailaer Basin. *Pet Geol Recover Effic* 18(3):20–23. <https://doi.org/10.3969/j.issn.1009-9603.2011.03.005>
- Dou LR, Wang RC, Wang JC, Cheng DS, Green PF, Wei XD (2021) Thermal history reconstruction from apatite fission-track analysis and vitrinite reflectance data of the Bongor Basin, the Republic of Chad. *AAPG Bull* 105(5):919–944. <https://doi.org/10.1306/11182019167>
- Douglas WW (2001) Mechanisms for generating overpressure in sedimentary basins: a reevaluation: Discussion. *AAPG Bull* 85(12):2118–2118
- Duddy IR, Green PF (2006) The role of apatite fission track analysis (AFTA) in constraining denudation histories. *Geochim Cosmochim Acta* 70(18-Sup1):A150a–A1150. <https://doi.org/10.1016/j.gca.2006.06.317>
- Du YM (2005) Dynamics of coal-formed gas reservoir formation in Huimin Depression. Geological Press. Beijing 50–53 (in chinese)
- Ferreira FAV, Barbalho TCS, Araújo IRS, Oliveira HNM, Chivavone-Filho O (2018) Characterization, pressure–volume–temperature properties, and phase behavior of a condensate gas and crude oil. *Energy Fuels* 32(4):5643–5649. <https://doi.org/10.1021/acs.energyfuels.8b00469>
- Gao G, Dong YX, Yang SR (2017) Genetic types and exploration field analysis of natural gas in Nanpu sag. *China Pet Explor* 22(6):16–26. <https://doi.org/10.3969/j.issn.1672-7703.2017.06.003> (in chinese)
- Guo RC, Li YJ, Li ZP, Gao SJ, Li WT, Yang XC (2010) The Reservoir formation model and main controlling factors of condensate oil/gas reservoir of the lower segment of Es4 in the Northern Part of the Dongying Sag. *Earth Environ*, 38 (2): 146–150. <https://doi.org/CNKI:SUN:DZDQ.0.2010-02-004>. (in chinese)
- Guo XZ, Zhang LP (2017) Maturity characteristics of the main humic-type condensate gas reservoirs. *Pet Geol Oilfield Dev Daqing* 36(2):39–44. <https://doi.org/10.3969/J.ISSN.1000-3754.2017.02.006> (in chinese)
- Huang GP, Zhang JB, Xiao B, Hong Y, Hao H (2003) Analysis of deep geologic characteristic of condensate reservoir in Baimiao Area. *Fault-Block Oil Gas Field* 10(3):16–18. <https://doi.org/10.3969/j.issn.1005-8907.2003.03.005> (in chinese)

- Jia R, Fu XF, Meng LD, Gong L, Liu ZD (2017) Transformation mechanism of fault and its associated microstructures for different kinds of reservoirs. *ACTA PETROL SIN* 38(3):286–296. <https://doi.org/10.7623/syxb201703005> (in chinese)
- Jiang YL, Wang X, Yu QQ, Wang YS, Liu H, Jing S (2016) Pressure field characteristics of petroliferous depressions and its relationship with hydrocarbon enrichment in Bohai Bay Basin. *ACTA PETROL SIN* 37(11):1361–1369. <https://doi.org/10.7623/syxb201611004> (in chinese)
- Lan CL, He SL, Zhang JF, Men CQ (2007) Discussion on the factors of controlling the distribution of the reservoir “sweet spots” of Sulige Gasfield. *J Xi’an Shiyou Univ (Natural Science Edition)* 22(1):45–48. <https://doi.org/10.3969/j.issn.1673-064X.2007.01.011> (in chinese)
- Li HB, Wang TG, Li MJ (2013) Tracing study on oil-gas filling pathways of Yakela gas condensate field in Tabei uplift. *Acta Petrol Sin* 34(2):219–224. <https://doi.org/10.7623/syxb201302002> (in chinese)
- Li JS (2013) Discovery and geological significance of high quality source rock in Bei'er sag of Hailaer Basin, China. *J Chengdu Univ Technol (Science & Technology Edition)*, 40 (3) : 326–332. <https://doi.org/10.3969/j.issn.1671-9727.2013.03.13>. (in chinese)
- Li XD (1998) Genetical types and formation model of condensate gas pools. *Geol Rev*, (2): 200–205. <https://doi.org/CNKI:SUN:DZLP.0.1998-02-015>. (in chinese)
- Li Y, Cao DY, Wei YC, Wang AM, Zhang Q, Wu P (2016) Middle to low rank coalbed methane accumulation and reservoiring in the southern margin of Junggar Basin. *Acta Pet Sin* 37(12):1472–1482. <https://doi.org/10.7623/syxb201612003>
- Liu HY, Huang BJ, Tuo L, Liang G, Xu XD (2018) Maturity discrimination and genesis analysis of condensate in the deep water gas fields of Qiongdongnan basin. *China Offshore Oil Gas* 30 (6):33–40. <https://doi.org/CNKI:SUN:ZHSD.0.2018-06-004>. (in chinese)
- Liu JX, Wang X, Wu HS, Hu W, Huang XG (2017) Identification method for condensate gas and light oil by gas logging and its application. *Spec Oil Gas Reserv* 24(5):48–53. <https://doi.org/10.3969/j.issn.1006-6535.2017.05.009> (in chinese)
- Lu K, Hou DJ, Hong HF, Cao HM (2010) Geochemical characteristics of crude oil and correlation of oil source in Huhuhu Sag. *J Guilin University Technol* 30(1):28–32. <https://doi.org/10.3969/j.issn.1674-9057.2010.01.004> (in chinese)
- Lu SF, Wang ZW, Huang DF, Zhao DX, Liu XY (1993) Hydrocarbon generation kinetics of coal rock macerals. *Science In China (Series B)*, 25(1): 101–107. <https://doi.org/CNKI:SUN:JBXX.0.1995-01-015>. (in chinese)
- Lu SF (1996) Kinetic theory of hydrocarbon formation of organic matter and its application. *Petroleum Industry Press, Beijing*, pp 56–61
- Nasriani HR, Borazjani AA, Sinaei M, Hashemi A (2014) The effect of gas injection on the enhancement of condensate recovery in gas condensate reservoirs: a comparison between a synthetic model and PVT cell results. *Pet Sci Technol* 32(5):593–601. <https://doi.org/10.1080/10916466.2011.596890>
- Osborne MJ, Swarbrick RE (1997) Mechanisms for generating overpressure in sedimentary basins: a reevaluation. *AAPG Bull* 81:1023–1041
- Ping HW, Chen HH, Song GQ, Liu HM (2012) Accumulation history of the deeply buried condensate reservoir in Minfeng sag of the northern Dongying depression and its exploration significance. *Acta Pet Sin* 33(6):970–977 (in chinese)
- Shen WJ (2010) Geochemical characteristics and the origin of gas from he10 well, Huhuhu depression in Hailar basin. *Nat Gas Explor Dev* 33(3):22–25. <https://doi.org/10.3969/j.issn.1673-3177.2010.03.007>
- Su Z, Zhang HF, Han JF, Liu YF, Sun Q, Bai Y, Duan YJ, Qu Y (2018) Origin and controlling factors of Mesozoic-Cenozoic gas condensates with high wax content and high-gravity oil in Kuqa Depression. *Oil Gas Geol* 39 (6) : 1255–1269. <https://doi.org/CNKI:SUN:SYYT.0.2018-06-016>. (in chinese)
- Sun XL, Wan YL, Liu ZW, Dong ZJ, Xiao QL (2013) Effects of natural evaporation on C5–C8 light hydrocarbon indicators: evidence from experimental results in the laboratory. *Acta Petrol Sin*, 34 (6): 1060–1069. <https://doi.org/CNKI:SUN:SYXB.0.2013-06-004>. (in chinese)
- Tissot BP, Wehe DH (1984) *Petroleum formation and occurrence*. New York, Heidelberg: Springer Verlag:121–143
- Tong XG, Zhang GY, Wang ZM, Wen ZX, Tian ZJ, Wang HJ, Ma F, Wu YP (2018) Distribution and potential of global oil and gas resources. *Pet Explor Dev* 45(4):727–736
- Wang WL (2007) Formation conditions of deep-seated condensate gas reservoir in the Paleogene in Dongying Sag. *Pet Geol Recover Effic* 14(3):55–57. <https://doi.org/10.3969/j.issn.1009-9603.2007.03.016>
- Wang WY, Pang XQ, Wu LY, Chen DX, Huo ZP, Pang Y, Chen D (2015) Pressure distribution features of deep and middle-shallow hydrocarbon reservoir in global oil and gas-bearing basins. *Acta Pet Sin* 36(S.2):194–202. <https://doi.org/10.7623/syxb2015S2018> (in chinese)
- Wang ZL, Xiao SD, Wang FL, Tang GM, Zhu LW, Zhao ZL (2021) Phase behavior identification and formation mechanisms of the BZ19-6 condensate gas reservoir in the deep Bozhong Sag, Bohai Bay Basin, Eastern China. *Geofluids*, 2021(0):1–19. <https://doi.org/10.1155/2021/6622795>
- Wei GQ, Xie ZY, Li J, Yang W (2017) New research progress of natural gas geological theories in China during the 12<sup>th</sup> Five-Year Plan period. *Nat Gas Ind* 37(8):1–13 (in chinese)
- Wu XD, Lv YP, Ma HY, Li LW, Feng H (2007) Study on effect of porous media on dew point pressure of condensate gas. *Pet Geol Oilfield Dev Daqing* 26(2):67–70. <https://doi.org/10.3969/j.issn.1000-3754.2007.02.017> (in chinese)
- Wu ZT, Wang YD, Liu XW, Zheng YW, Zheng JJ (2017) Natural gas accumulation process and main controls factors of Hutubi condensate gas field. *Contrib Geol Mineral Resour Res* 32(3):403–408. <https://doi.org/10.6053/j.issn.1001-1412.2017.03.008> (in chinese)
- Xu H, Zhang JF, Tang DZ, Yi W, Chen YP, Lin WJ (2009) The study status and tendency of low pressure oil and gas reservoir. *Adv Earth Sci*, 24(5):506–511. <https://doi.org/CNKI:SUN:DXJZ.0.2009-05-010>. (in chinese)
- Xue YA, Li HY (2018) Large condensate gas field in deep Archean metamorphic buried hill in Bohai sea: discovery and geological significance. *China Offshore Oil Gas* 30(3):1–9. <https://doi.org/10.11935/j.issn.1673-1506.2018.03.001>
- Yang DB, Zhu GY, Liu JJ, Su J, Zhang B, Fei AG (2010) Distribution of global condensate gas field and major factors controlling its formation. *Earth Sci Front*, 17 (1): 339–349. <https://doi.org/CNKI:SUN:DXQY.0.2010-01-033>. (in chinese)
- Yang HJ, Zhu GY (2013) The condensate gas field geological characteristics and its formation mechanism in Tarim basin. *Acta Petrol Sin*, 29(09):3233–3250. <https://doi.org/CNKI:SUN:YSXB.0.2013-09-022>. (in chinese)
- Zhang F (2014) Geochemical characteristics and hydrocarbon-generating potential of coal-bearing source rock with middle to low coal rank, Huhuhu depression. *Nat Gas Explor Dev* 37(2):19–23. <https://doi.org/CNKI:SUN:JHSX.0.2014-07-004> (in chinese)
- Zhang GC, Zeng QB, Su L, Yang HC, Chen Y, Yang DS (2016) Accumulation mechanism of LS 17\_2 deep water giant gas field in Qiongdongnan Basin. *Acta Pet Sin* 37(S.1):34–36. <https://doi.org/10.7623/syxb2016S1004> (in chinese)
- Zhang WZ, Guo YR, Tang DZ, Zhang JF, Li M, Xu H, Lin WJ, Tao S (2009) Characteristics of fluid inclusions and determination of gas accumulation period in the Upper Paleozoic reservoirs of Sulige

- Gas Field. *Acta Pet Sin* 30(5):685–691. <https://doi.org/10.3321/j.issn:0253-2697.2009.05.009> (in chinese)
- Zhao JZ, Li J, Xu ZY (2017) Advances in the origin of overpressures in sedimentary basins. *Acta Petrol Sin*, 39 (9): 973–998. <https://doi.org/CNKI:SUN:SYXB.0.2017-09-001>. (in chinese)
- Zhou XX, Li SJ, Chen YC (1996) Formation of Condensate gas pools in Tarim basin. *Pet Explor Dev*, 23( 6) : 7–11. <https://doi.org/CNKI:SUN:SKYK.0.1996-06-001>. (in chinese)
- Zhu GY, Yang HJ, Zhang B, Su J, Chen L, Lu YH, Liu XW (2012) The geological feature and origin of Dina 2 large gas field in Kuqa Depression, Tarim Basin. *Acta Petrol Sin*, 28 (8): 2479–2492. <https://doi.org/CNKI:SUN:YSXB.0.2012-08-016>. (in chinese)